The organization of cholesteric spherulites

Y. Bouligand, F. Livolant

J. Physique **45** (1984) 1899-1923 DÉCEMBRE **1984,** PAGE 1899

Classification
Physics Abstracts
61.30E — 61.70

The organization of cholesteric spherulites

Y. Bouligand and F. Livolant

E.P.H.E. and C.N.R.S., 67, rue Maurice-Günsbourg, 94200 Ivry-sur-Seine, France

(*Reçu le 11 avril 1984, accepté le 21 août 1984*)

Résumé. — Les germes cristallins liquides cholestériques ont été étudiés avec des produits nématiques (MBBA, PAA) torsadés par le benzoate de cholestérol et également avec différents polymères d'intérêt biologique : un polypeptide de synthèse (le PBLG), un acide nucléique (l'ADN) et un polysaccharide (le xanthane). Il existe des germes sphériques ou allongés présentant une orientation uniforme des couches, des sphérulites à couches concentriques possédant le plus souvent un rayon de disinclinaison et des sphérulites intermédiaires entre ces deux types. Dans la masse du germe, les orientations moléculaires sont continues, même en présence d'un rayon de disinclinaison et nous présentons dans ce cas un modèle continu du cœur de la disinclinaison. La topologie d'ensemble des germes est discutée et modélisée. Les seules discontinuités que l'on peut rencontrer sont localisées à l'interface et seulement dans le cas de conditions angulaires strictes. Une revue des sphérulites existant dans les structures biologiques est également présentée.

Abstract. — Germs of cholesteric liquids were studied in classical mixtures of nematic compounds (MBBA, PAA) with a twisting substance (cholesterol benzoate). These germs were also studied with different polymers of biological interest : synthetic polypeptides (PBLG), nucleic acids (DNA) and polysaccharides (xanthan). Germs are either spherical or elongated with a uniform orientation of layers; there are spherulites which are intermediate between these two types. The molecular orientations are continuous in the bulk of all germs, even in the presence of a disclination radius. In this case a continuous model of the disclination core is presented. The whole topology of germs is discussed and modelled. The only discontinuities are to be found at the interface only in the case of definite angular conditions. The occurrence of spherulites in biological systems is reviewed.

1. Introduction.

Cholesteric spherulites and rodlets were first described by Lehmann [1] and Friedel [2] in slowly cooled isotropic phases of components such as cholesterol benzoate. Spherical nematic germs were also studied by these authors. More recent works on synthetic polypeptides and, in particular, on poly-γ-benzyl-L-glutamate (PBLG) showed remarkable pictures of spherulites [3] and their structure was modelled by Pryce and Frank [4]. Polymers such as polyethylene present a spherulitic crystallization, whose texture is very close to that of cholesteric droplets, though these polyethylene spherulites correspond to a true crystalline state (see bibliography in Keller, [5]).

This article deals with several kinds of spherulites or rodlets given by various nematic and cholesteric components, some of them having a biological origin : double helical deoxyribonucleic acid and Na-xanthan, a bacterial polysaccharide; these two polymers were observed in concentrated aqueous solutions. We re-examined the synthetic polypeptide studied by Robinson [3, 6], namely poly-γ-benzyl-L-glutamate, forming cholesteric solutions in dioxan. The cholesteric droplets which appear at transition were compared to those given by MBBA (methoxy-benzylidene-butylaniline) or PAA (paraazoxyanisol), these nematic compounds being studied pure or with added cholesterol benzoate or another twisting agent. These comparative observations allow us to restudy all the varieties of the spherulites described so far and rodlets and to discuss their occurrence in biological systems. Intermediate forms exist between different types of spherulites and new models are proposed. We present a large series of tridimensional reconstructions to clarify the organization of these spherulites which are often difficult to visualize globally.

Textures which appear from an isotropic transition result in general from the coalescence of spherulites and a good knowledge of germs is necessary to understand the distribution of defects.

2. Materials and methods.

The chemical formulae of the various mesogens used in this study are reviewed in table I, the double helical DNA being excepted, its chemical description being too long, but presented in innumerable books (see Alberts *et al.* [7]).

a) DNA. Calf thymus DNA (Merck) solution (50 mg in 50 ml of 15 mM Tris Cl^- buffer, at pH 8, magnetically stirred during 24 h), was sonicated for different times ranging from 5 to 35 s by successive pulses of 5 s separated by intervals of 15 s, with a Branson sonifier B 15 P (20 kHz, 50 W), the solution being kept at 0 °C. DNA was precipitated in ethanol and air dried. The differently sonicated DNA were solubilized in 10 mM Tris Cl^- buffer at pH 8 (1 mg/ml of DNA in buffer) and KCl was added to such concentrated DNA solutions. A drop of this mixture was deposited between slide and coverslip and the preparations were stored at 0 °C. The cholesteric structure organizes progressively and is clearly recognizable approximately a week later. Good preparations were obtained one or two months later, the best concentrations being 10 mg/ml DNA and 0.4 M KCl. This procedure is derived from those of Robinson [8].

b) PBLG. This polymer synthesized in Orleans, Centre de Biophysique Moléculaire, was dissolved in dioxan. The solution was progressively evaporated between slide and coverslip and cholesteric spherulites appeared floating in the isotropic phase.

c) Na-xanthan. This polymer secreted by *Xanthomonas campestris* was kindly provided by Drs. Rinaudo and Milas who purified this material [9]. This polysaccharide gives a cholesteric phase when dissolved in distilled water or in 6 % NaCl solution [10].

d) MBBA and PAA. Nematic droplets of MBBA or PAA, twisted by a small amount of cholesterol benzoate were observed floating in the isotropic phase, by increasing temperature or by addition of a solvent such as toluene. Droplets were also observed by suspending these nematic or cholesteric phases in glycerol.

All preparations were observed with a Leitz polarizing microscope (Orthoplan-Pol), either in natural light or between crossed polars or between opposite circular polarizer and analyser.

Table I. — *Structure of the different molecules and polymers used in this study.*

Poly-γ-benzyl-L-glutamate (PBLG)

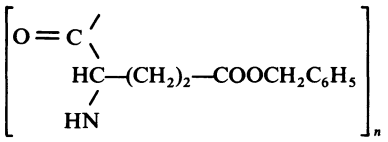

Xanthan

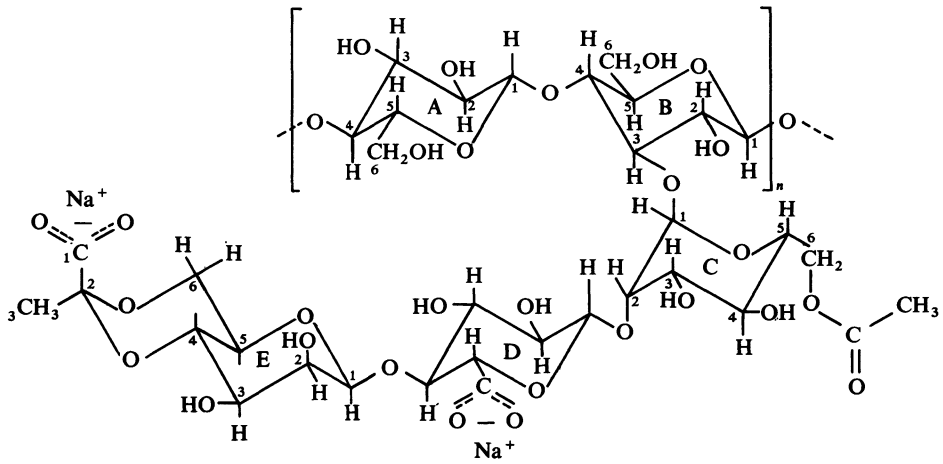

Methoxy-benzylidene-butylaniline (MBBA)

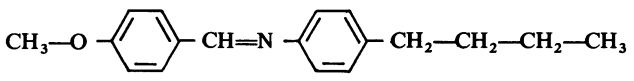

Paraazoxyanisol (PAA)

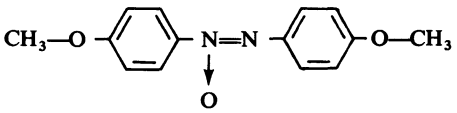

3. Observations.

3.1 GENERAL ASPECTS. — We first summarize our observations to give a general idea of cholesteric droplet morphologies. The droplets belong to either of the three general classes.

3.1.1. *Cholesteric layers show a uniform or an almost uniform orientation in the droplet.* — A variable angle α separates the cholesteric layers from the interface, α being often close to 90°. This situation is represented in figure 1 a-d. When germs are small, they show generally a spherical shape (a). Layers lie at right angle to the interface along the equator, whereas they are tangent at the two opposite poles. In between, α varies regularly. When germs grow, they often elongate (b, c). The orientation is uniform in (b), whereas layers are bent in (c) to keep a normal orientation of layers relative to the interface. In (d) we indicate a frequent appearance of these droplets (round or elongated), when the cholesteric axis is oblique. The observed spiral is a surface structure of the germ which is analysed below.

3.1.2 *Cholesteric layers are parallel or almost parallel to the interface and show a radial distribution of cholesteric axes.* — The angle α is thus small in most regions of the interface. This situation is represented in figure 1e-i. Spherulites with concentric layers present either a *singular radius*, which is a frequent situation (e), or a *singular diameter*, which is not frequent (f), or a *curved singular line*, which is rare (g). When these singular lines are oriented vertically (i.e. in the direction of the microscopic axis), one observes either *double spirals* (h) for the (e) type and, possibly, for the (f) and (g) types or *concentric circles* (i) for the (f) and (g) types. These series of concentric lines are well contrasted, when the microscope is focused on the centre of spherulites; layers are then examined in vertical position and the image is very sharp.

3.1.3 *There are other types of spherulites, which can be considered as intermediate* (Fig. 1j-l). The spherulite shown in figure 1j is obtained from that represented in figure 1a by a simple deformation. Each layer, instead of being flat is transformed into a cup and the spherulite resembles then a series of nested cups. If the deformation is pursued, some of the cups become closed and a radial singularity arises (Fig. 1k). When observed in cross section (perpendicularly to the common axis of the cups), one observes double spiralized patterns as in figure 1h. Another type of spherulite presents more or less cylindrical layers (Fig. 1l), but this structure will be discussed below.

It is worthy of note that certain spherulites can be flattened between slide and coverslip. This is diagrammatically shown in figure 2a, b for a spherulite with a horizontal singular radius. Between slide and coverslip (hatching), the double spiralized pattern is extended horizontally, so that a large central zone is formed of horizontal cholesteric layers and appears black between crossed circular polarizers.

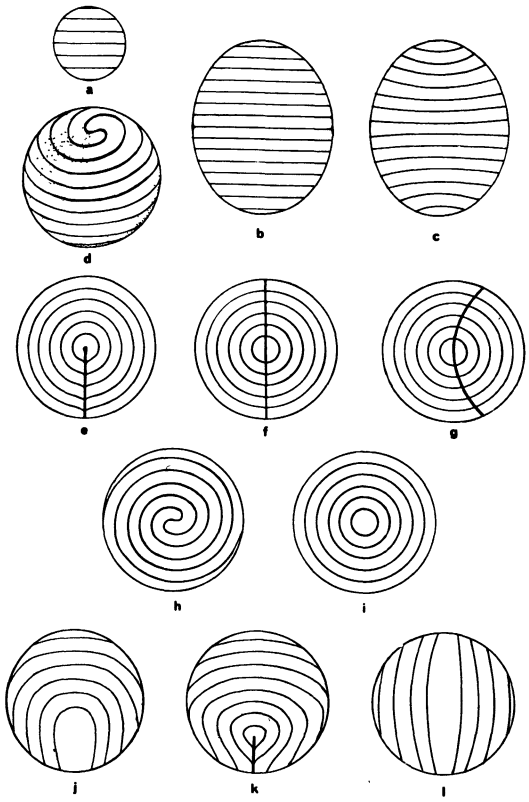

Fig. 1. — Schematic representations of cholesteric droplets encountered in these studies. Cholesteric layers are indicated by parallel equidistant lines (separated by the half helicoidal pitch).
a. Spherulite with a uniform orientation of the cholesteric axis.
b. Elongated germ, with a uniform orientation of layers; the elongation axis is parallel to the cholesteric axis.
c. Elongated germ with layers lying normally to the interface.
d. Surface aspects of a spherical germ with uniformly oriented layers, the cholesteric axis being oblique; the double spiralized pattern forming at one of the two poles is visible at the upper interface.
e. Spherulite with concentric layers showing a horizontal disclination radius (parallel to the preparation plane).
f. Spherulite with concentric layers, showing a horizontal disclination diameter.
g. Spherulite with concentric layers and a disclination arc, topologically equivalent to a disclination diameter.
h. Spherulite showing a double spiralized pattern in its equatorial plane. This aspect can be that of spherulites e, f when the disclination line is oriented vertically.
i. Spherulite with concentric layers in its equatorial plane, this picture being observed with certain spherulites such as f or g; the disclination line is vertical.
j. Spherulite with a configuration intermediate between c and e.
k. The spherulite j can transform into that represented in k with a short disclination radius.
l. Spherulite with layers almost parallel to one diameter; in cross section, such a spherulite may give either a double spiralized pattern (h) or a concentric pattern (i).

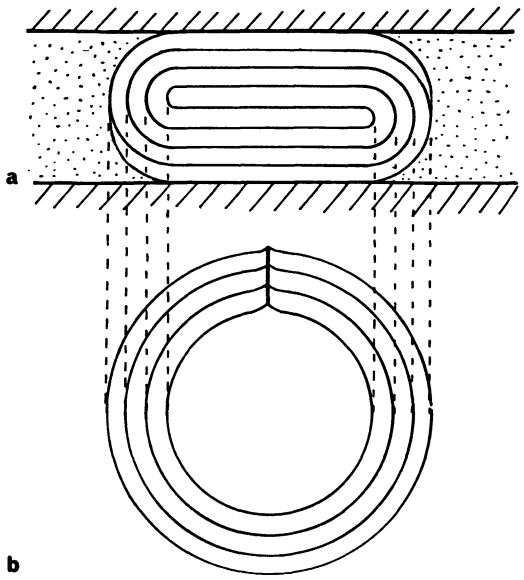

Fig. 2. — Spherulite sandwiched between slide and coverslip. This spherulite is represented in side-view (a) or in top view (b). Its structure is that presented in figure 1e and h, but the spiral pattern is flattened here.

All these morphological aspects of germs are illustrated in plates I to V. Plate I shows PBLG spherulites, which are either free in the isotropic phase (b, c) or flattened between slide and coverslip (a) or attached only to one glass (g, h, i). Plate II presents various xanthan spherulites and plate III the examples of DNA germs, limited either by the isotropic solution (a, d, e) or by air (b, c). In the following plates are presented the spherulites obtained with classical nematic liquid crystals twisted with cholesterol benzoate : MBBA in plate IV and PAA in plate V.

Germs attached only to one glass present in general an architecture which is often very different from that of free spherulites or those sandwiched between slide and coverslip. These germs generate the classical « Schlieren texture » with numerous nuclei (Maltese crosses around vertical directors or thin vertical threads surrounded by two black brushes) and with ribbons representing the locus of horizontal directors. Such textures were studied in Bouligand [11]. In certain cases germs are almost nematic (xanthan, Pl. IIg, PBLG also in some preparations). For xanthan the pitch depends strongly on ionic conditions, which are not well controlled.

3.2 DETAILED OBSERVATIONS. — In the following considerations, slide and coverslip define the horizontal plane. The microscope axis is therefore vertical.

3.2.1 *Layers normal or oblique to the interface : germs with uniform orientation of layers.* — Examples were found in concentrated aqueous solutions of DNA (Pl. IIIa, e), in cholesterized MBBA (Pl. IVc, d, e, f) and in cholesterized PAA (Pl. Va). When the cholesteric axis is horizontal (parallel to slide and coverslip), layers are vertical and show a uniform thickness (Pl. IVc). When the helicoidal pitch is sufficiently high, an oblique view or an axial view of these germs shows a surface double spiral, well visible in plate IVf. Each pole presents such a double spiral.

These cholesteric droplets forming from the isotropic phase, are generally spherical at the beginning of the mesomorphic transition and elongate later. One observes elliptical germs (Pl. IVd) when the transition progresses. If one reheats germs of twisted MBBA, they transform into rods, with more or less cone-shaped ends, instead of being rounded (Pl. IVe). These cholesteric droplets are often sandwiched between slide and coverslip and this is probably the case of figures d and e in plate IV and the case of most spherulites in plate V. In order to know whether or not a germ is free in the isotropic phase, one can shift slightly the coverslip and observe the behaviour of germs. Changing the focus also suffices, in thick preparations, to make sure of this.

In such spherulites, layers are normal to the interface along the equator, they are parallel at the two poles and oblique in between. The parallelism between the elongation axis and the cholesteric axis indicates an anisotropy of the surface energy, which is lower when layers lie normally to the interface (Pl. IVd, e). Around the two poles, layers show in some spherulites a concavity oriented outwards. This deformation makes the layers closer to the orientation perpendicular to the interface. The layer thickness is altered in such regions, layers are slightly thicker near the interface around the two poles.

The rod-shaped germs observed in concentrated DNA solutions (Pl. IIIa, d, e) resemble the chromosome structure studied in certain microorganisms [12].

3.2.2 *Layers parallel to the interface : spherulites with more or less concentric layers.* — This parallelism draws its origin from the parallelism of molecules themselves with the interface, in its close vicinity. Since the droplets are generally spherical, particularly when they are very small, the parallel cholesteric layers are forced to adopt a concentric arrangement well illustrated by PBLG spherulites (Pl. Ia-e). The cholesteric germs grow in concentrated solutions of this synthetic polypeptide in dioxan or in other organic solvents. The structure is well observed between crossed circular polarizers (Pl. Ia-d) and one recognizes three different patterns that we call respectively *double spirals* (Pl. Ia, c), *concentric tear-drops* (Pl. Ia, b) and *concentric rings* (Pl. Id, f). They correspond to sketches of figure 1h, e, i.

The bright lines which are well focused, half way from slide to coverslip, form double spirals which show both orientations clockwise and anticlockwise (compare the two smallest spherulites of Pl. Ia). One also observes spherulites presenting a series of concentric tear-drop-shaped lines. These bright lines are closed and concentric; they show a series of cusps aligned along a singular radius of the spherulite. The aspect

of tear-drop originates from these cusps. The spherulites can be moved by a slight shift of the coverslip and this shows how double spiralized patterns transform into tear-shaped ones and conversely. This morphology was described by Robinson [3] and interpreted according to a model due to Pryce and Frank, presented in an appendix to the work of Robinson *et al.* [4]. We analyse below this model and its refinements.

Such spherulites often coalesce and this leads to the presence of defects which are generally $\lambda^{-\pi}$ disclinations (Pl. Ik, l; Pl. IIf). In several isolated spherulites and in aggregated spherulites, one observes sometimes a central black area which indicates, as quoted above, that the system is sandwiched between slide and coverslip (Pl. Ia, b, d, k).

When MBBA is slightly cholesterized with cholesterol benzoate, one can get beautiful spherulites if the mesophase is dispersed in glycerol. The layers are parallel to the interface and most of the spherulites show either the double spiral (Pl. IVj) or a singular radius (Pl. IVi). The helicoidal pitch varies as the inverse of the cholesterol benzoate concentration in MBBA and it is possible to have very large pitches. In these conditions, the spherulite shows a series of nested tear-drops (Pl. IVh) and one sees clearly that the radial singularity is formed by a set of cusps showing a discrete translational symmetry. We observed one spherulite with only one tear-drop (Pl. IVg).

In xanthan, as already reported by Milas, the double spiralized spherulites are frequently observed (Pl. IIc) with their singular radius (Pl. IId). They show therefore a geometry very similar to that of spherulites described by Robinson in PBLG [3]. Some rare spherulites with a singular diameter were also observed in this material (Pl. IIe) but pictures were not well resolved; they probably present concentric layers in equatorial section as it will be suggested in models discussed below. However, most xanthan spherulites with concentric layers (Pl. IIa 3) probably correspond to an intermediate type.

As indicated above, cholesteric layers are parallel to the interface, and this is probably due to the parallelism of the polymer itself to the interface. There are spherulites which are almost nematic with a very low twist and one sees also that the interface is illuminated between crossed polars, when it lies at 45° to the directions of polarization and is black when parallel to these directions. This shows directly that this alignment of molecules at the interface is not due to the twist.

Some spherulites of cholesterized MBBA suspended in glycerol present a curved singular diameter, but they are extremely rare (Pl. IVl). Another example is very interesting and shows a ring with two singular points (Pl. IVk). One also observes rare cases of spherulites with closed rings (Pl. IVm) as described above in xanthan.

Other examples of spherulites showing layers parallel to the interface were found in concentrated aqueous solutions of DNA. The interface separates either the mesophase from the isotropic phase (Pl. IIIa) or the mesophase from air (Pl. IIIb). In this last example, the observed structure is not a spherulite since it is a very small droplet joining slide and coverslip.

3.2.3 *Intermediate spherulites.* — Germs with oblique layers (at an angle α, far from 0° or 90°) are not rare and examples are shown on plates I (f, j), III (a), IV (n, o), V (a, b, c). We already considered the spherical germ with uniform orientation of the cholesteric axis, which shows two large zones of obliquity at the interface (Pl. IVc). One also finds germs in PBLG solutions in which one part of the droplet is formed by concentric or spiralized layers, whereas the rest of the germ resembles a rodlet (Pl. If, j). One should note that these examples correspond to flattened germs, sandwiched between slide and coverslip; the layers lie therefore almost perpendicular or oblique to the glass boundary in contrast with other PBLG spherulites shown in plate I (a, b) and schematized in figure 2. We do not know the reason of this particular and rare behaviour.

Some spherulites of PBLG (Pl. Ie) and a non negligible proportion of those observed in xanthan show an almost concentric arrangement of layers. However, instead of showing a singular diameter as in figure 1f, layers are oblique in the vicinity of the poles, as represented in figure 1l.

Germs of cholesteric DNA also show situations intermediate between concentric layers and aligned flat layers. An example is observed in the left part of micrograph a in plate III and in micrograph d of the same plate.

Germs with a small number of layers often show large areas of obliquity at the interface. This is the case of spherulites n and o in plate IV, and this situation is very general. The obliqueness of layers, even very slight, never completely disappears in spherulites with concentric patterns and many more layers (see Pl. IIc; Pl. IVi, j).

A beautiful intermediate structure is that observed in PAA doped with cholesterol benzoate. Many spherulites show an almost uniform orientation of the cholesteric axis. The layers are however more or less concave (Pl. Va). In certain spherulites, which have reached sufficiently large dimensions, some layers are engulfed by a process which resembles the gastrulation of an embryo. The invaginated layers form a singular line which is similar to the radius described above in PBLG spherulites and in twisted MBBA droplets. The shape of the nested tear-drops is variable and, in some spherulites, they form more or less curvilinear triangles (Pl. Vc). When the spherulites are not yet invaginated, they often present two regions which differ by the contrast. One easily verifies that layers of lower contrast are oblique relative to the microscope axis and present a larger periodicity, whereas the more contrasted ones are almost vertical and are therefore in a posi-

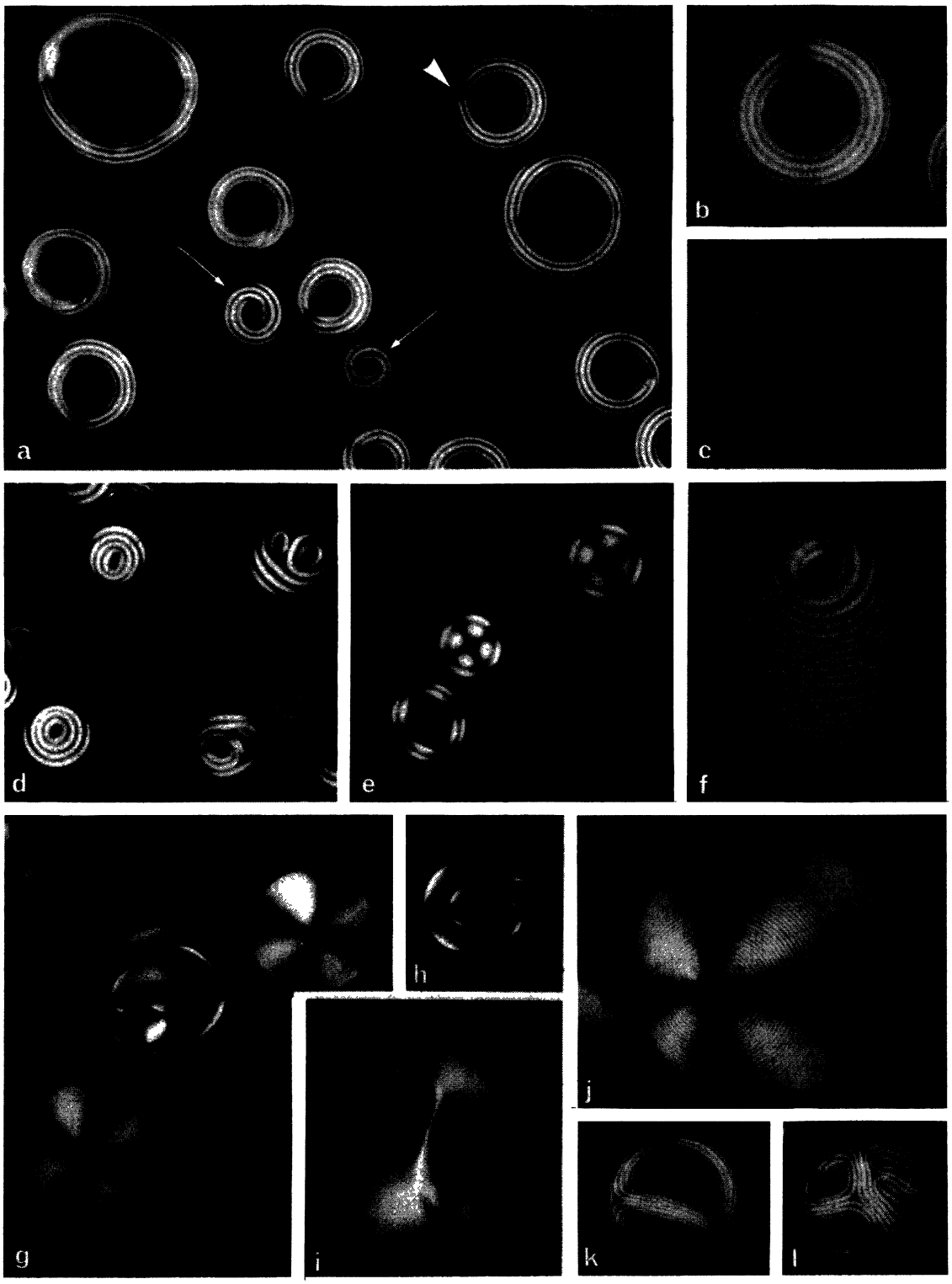

Plate I. — Cholesteric droplets of PBLG in equilibrium with the isotropic phase, observed between crossed linear polars (e, g, h, i, j) or between crossed circular polars. Certain spherulites are flattened between slide and coverslip and this is the case principally of figures a, b, f, j.

a, b, c : A first type of spherulites shows, according to the angle of observation, either a double spiralized pattern (a arrows, c) or a singular radius (a arrow heads, b). As a general rule, the cholesteric layers and molecules themselves tend to align parallel or nearly parallel to the interface. Observe however at the top of figure c layers which cut obliquely the isotropic interface (a : × 490 ; b : × 680 ; c : × 1 000).

d, e, f : Another type of spherulites shows concentric closed bright bands, well visible between crossed circular polars (d, f). Between crossed linear polars (e) are observed two types of black crosses, either with a small central black area (top right,

tion to form thick threads; these are known in nematics and in slightly twisted nematics to decorate the locus of vertical directors (parallel to the microscope axis).

4. Models.

4.1 Spherulites or rodlets with a uniform orientation of the cholesteric layers.

4.1.1 *Arced patterns in oblique section.* — In the absence of surface distortions, the cholesteric order is perfect and the director components are

$$n_x = \cos 2\,\pi z/p\,, \quad n_y = \sin 2\,\pi z/p \quad \text{and} \quad n_z = 0$$

p is the helical pitch and Oz the cholesteric axis, parallel to the long axis of the cholesteric germ, when this germ is elongated. However, such germs often remain spherical. The isotropic interface forms a sphere or an elongated revolution ellipsoid. This interface cuts the cholesteric layering obliquely and the directors at the interface project onto it along a series of nested arcs. This is easily understood from the fact that such series also form when the interface is a plane oblique to the cholesteric axis. The observed curves along which align the molecules observed in projection onto this plane are :

$$X = X_0 + \text{Log} \mid \sin S \mid$$

X and S being the coordinates along two normal axes chosen in this oblique plane, X being normal to z. X_0 is an additive constant, parametrizing the arcs. One has to choose appropriate units for X and S [13].

4.1.2 *Drawing conventions.* — With the classical nail convention of Kléman and Friedel [14] (1), the arrangement of directors in the oblique interface plane is represented in figure 3a. The distribution of nails can be replaced by a distribution of force lines (Fig. 3b) which are arrowed in the sense of the acute ends of nails. The locus of directors parallel to the interface is represented by a double line L. We have already used these conventions in previous works on cholesteric textures [11]. As observed in figures 3a, b, these double lines, representing the locus of directors parallel to the interface, coincide with the common asymptotes of the series of nested arcs. This situation is changed when one considers a spherical or an ellipsoidal interface for instance. This geometry is described in figures 3c, d with similar conventions (nails or arrowed force lines). In this case, the asymptotic curves A of the nested arcs do not coincide any more with the double lines L corresponding to the locus of interfacial directors tangent to the interface (Figs. 3c, d). The reader can try to prove it as an exercise, but this result will become obvious from the study of the following figures.

4.1.3 *Interface double spirals.* — Double spiral patterns are observed at the surface of these spherulites and rodlets as shown in plate IVf. These spiral patterns are diametrically opposite in the direction of cholesteric axis defining two poles P and P′ (the extremities of rodlets). The origin of these patterns is modelled as follows. Consider a spherulite or a rodlet along a meridian section (Fig. 4a). Molecules are aligned in successive horizontal discs of decreasing diameter. These discs are represented in a perspective view (Fig. 4b). The pattern observed in top view can be built with discs like that of figure 4c, of decreasing sizes, superimposed helically (Fig. 4d). The resulting double spiral is underlined in figure 4e. The arrow convention is used in figure 4f. This representation, as those of figure 3 uses two successive projections : the first one onto the interface which is spherical or ellipsoidal, and the second one onto the figure plane, along the cholesteric axis. In this model, series of parallel nested arcs form a double spiral. There are two different double spirals : one of them is represented by a thick line A which corresponds to the limit of series of arcs; this line A is an asymptotic curve for all arcs of the pattern. There is a second double spiral L, represented by a double line. This locus corresponds to directors at the interface, lying parallel to the interface. To have a good understanding of these spirals, the reader can build himself this model of the apex

(1) In this convention, molecular orientations are represented by segments, nails and points when molecules are respectively parallel, oblique or normal to the plane or to the surface on which they are drawn. Acute ends of nails correspond to molecular extremities pointing towards the observer.

centre), or with a large central area (bottom left); this second black cross opens into two hyperbolic branches by rotation of the microscope stage. The cholesteric layering of such droplets presents a revolution symmetry. This symmetry is broken by the interface in f where layers lie obliquely (d : × 780 ; e : × 490 ; f : × 1 100).

g, h, i : Droplets attached to one of the glasses limiting the preparation. Directors are vertical at the centre of Maltese crosses (g); the obliquity of the cross indicates a slight twist. The white line visible also in (h) and (i) corresponds to a narrow ribbon, locus of horizontal directors (× 865).

j, k, l : Droplets flattened between slide and coverslip, with various textures. j : Large, round and eccentric globule, with a very small cholesteric pitch. k : Two fused spherulites showing both a singular radius. l : Droplets resulting of the coalescence of four spherulites (j : × 530 ; k : × 370 ; l : × 430).

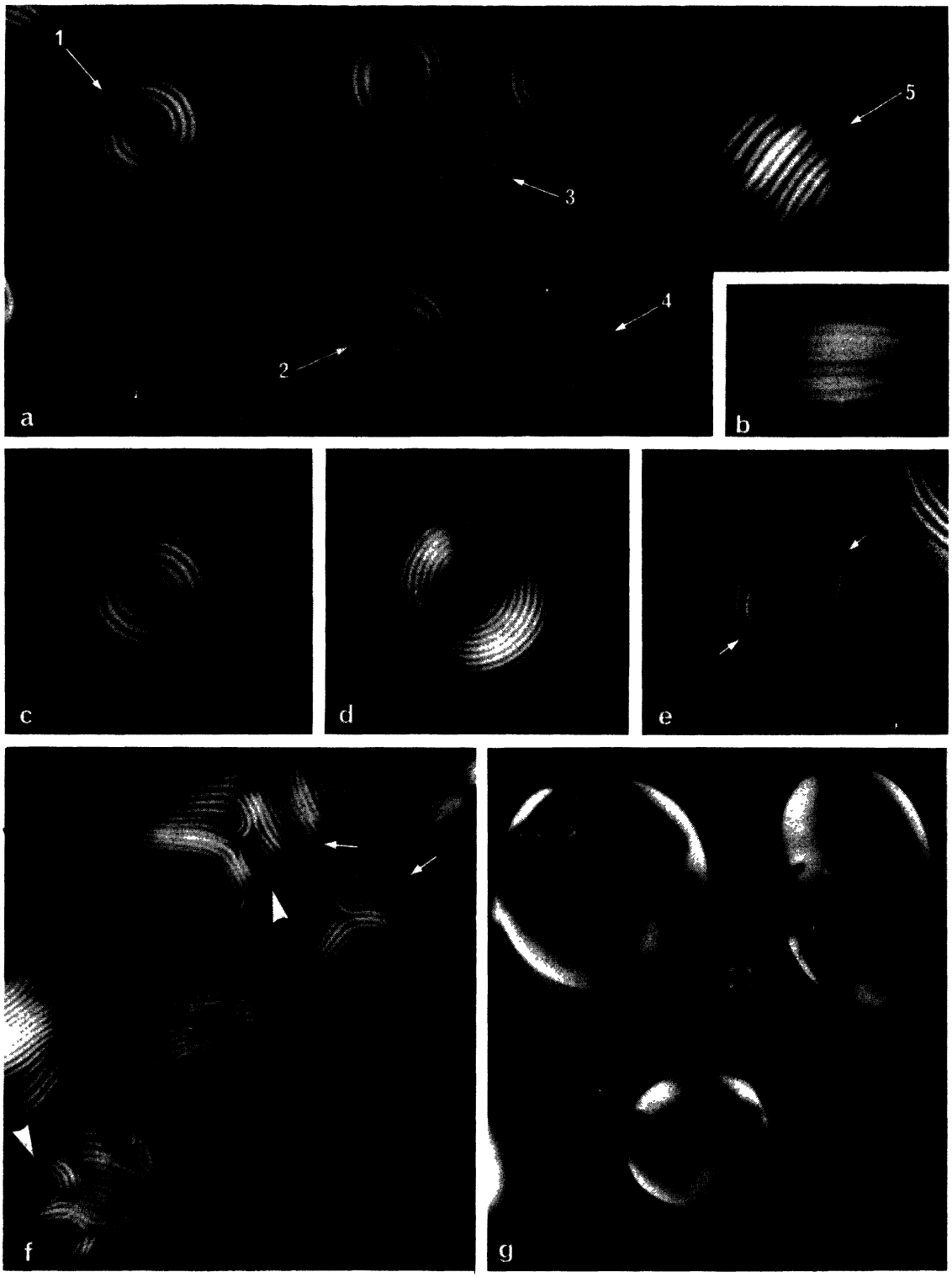

Plate II. — Spherulites of xanthan in equilibrium with the isotropic phase (NaCl or KCl solution + xanthan). Observations between crossed circular polars (a, b, c, d, e, f) or between crossed linear polars (g).

a. General view of several kinds of droplets showing different patterns : double spirals (1), concentric closed curves (2), more or less oblique orientations difficult to interpret (3); small spherulites (4); globule resulting from the coalescence of several spherulites (5) (× 1 100).

b. Globule with a double spiralized pattern, swept along by movements of the liquid. The shape is elongated but regains its structure when the motion ceases (× 1 230).

c. Globule showing a clear double spiralized pattern (× 990).

d. Spherulite showing a disclination radius (× 950).

e. Spherulite showing a disclination diameter; the two poles are indicated by arrows (× 1 180).

f. Composed globules; each subunit corresponds to one type already described, double spiralized pattern (arrow), concentric bands (arrow-head) (× 560).

g. Nematic globules observed in similar conditions (× 475).

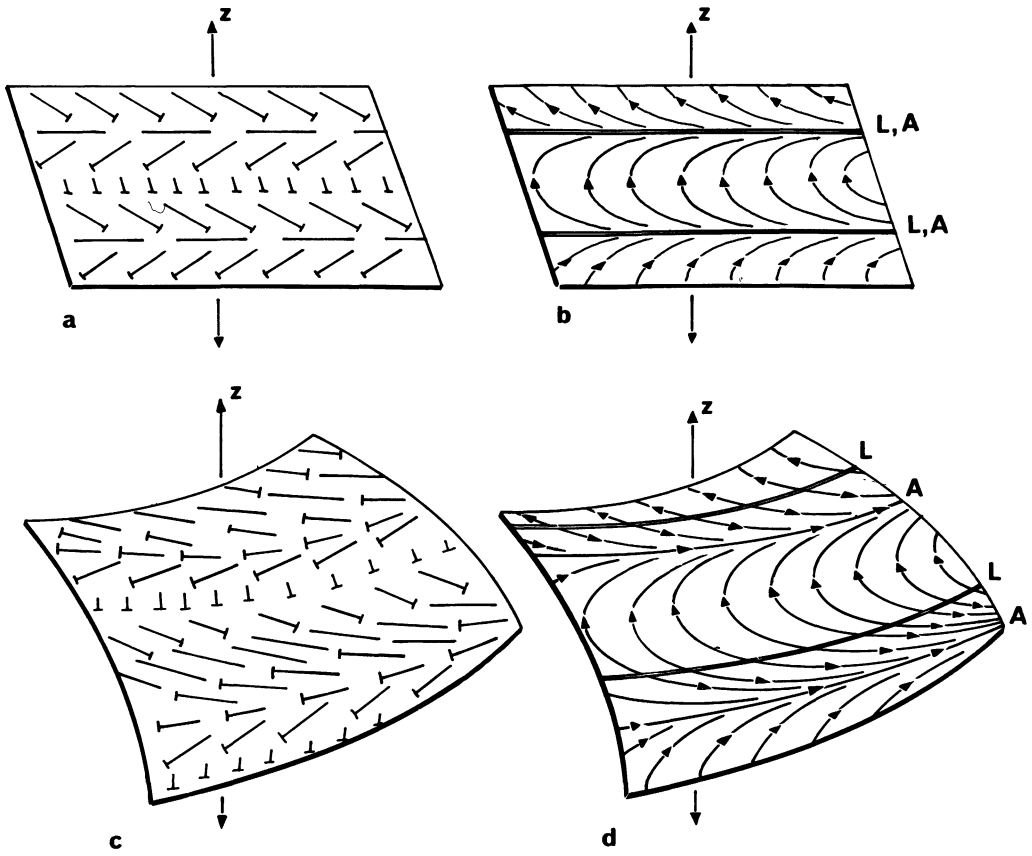

Fig. 3. — Conventions used to represent directors of a cholesteric liquid crystal within certain planes or surfaces. The axis z represents the cholesteric axis.
a. Nail convention applied to an oblique planar section.
b. Arrowed lines convention applied to the same planar section. The nails follow force lines which form parallel series of nested arcs. The asymptotes A are superimposed to lines L, locus of directors parallel to the section plane.
c. Distribution of nails within a curved surface.
d. Arrowed lines convention applied to figure c. The asymptotic lines A of the series of nested arcs do not superimpose to lines L. The arrow is reversed when a force line crosses a line L.

of the cholesteric rodlet ([2]). We speak below about the origin of this spiral pattern.

4.1.4 *Interface singularities.* — Another interesting region in such spherulites is that of the equator, defined as the largest circle normal to the cholesteric axis. This is represented in figure 5. We consider here the zone lying between two parallels symmetrical with respect to the equator. If these two parallels differ only by a small latitude angle, the circular ribbon formed by this zone can be cut along a meridian and spread onto the plane (with the help of slight deformations). The result of our study in this region is represented in figures 5b, c. There are two singular arrangements which correspond to the nail distribution around the two diametrically opposite points S and S′, where the

([2]) A set of parallel and equidistant lines can be drawn on a sheet of paper. It represents a thin layer of aligned molecules or polymers. This drawing is reproduced to get a large number of such sheets. A series of discs of decreasing size are cut in these sheets and superposed with a regular twist. The second disc is put onto the first one in a concentric position but rotated by a small angle relative to disc no. 1. Each disc presents two diametrically opposite points with directors parallel to tangent at these points and thus parallel to the interface. The helicoidal stack of discs makes that these two points describe around the pole P a double spiral, which is nothing else than the line L. Directors along L are normal to the corresponding radius, and since L is a spiral, these directors necessarily cut L obliquely. Besides, this construction reveals how the double spiral of arcs and their limiting double spiral A are formed. The double spiral L corresponds to an inversion of arrows along arcs. Along the line A directors are oblique relative to the corresponding radius and oblique relative to the interface, since they follow A in projection onto the interface. This indicates how the differenciation between lines A and L originates, along curved surfaces in general, this being not observed in planar sections (Figs. 3*c*, *d*). Playing with such a model is recommended to people working on cholesteric spiral patterns. It was presented in several anterior works [13, 16, 57].

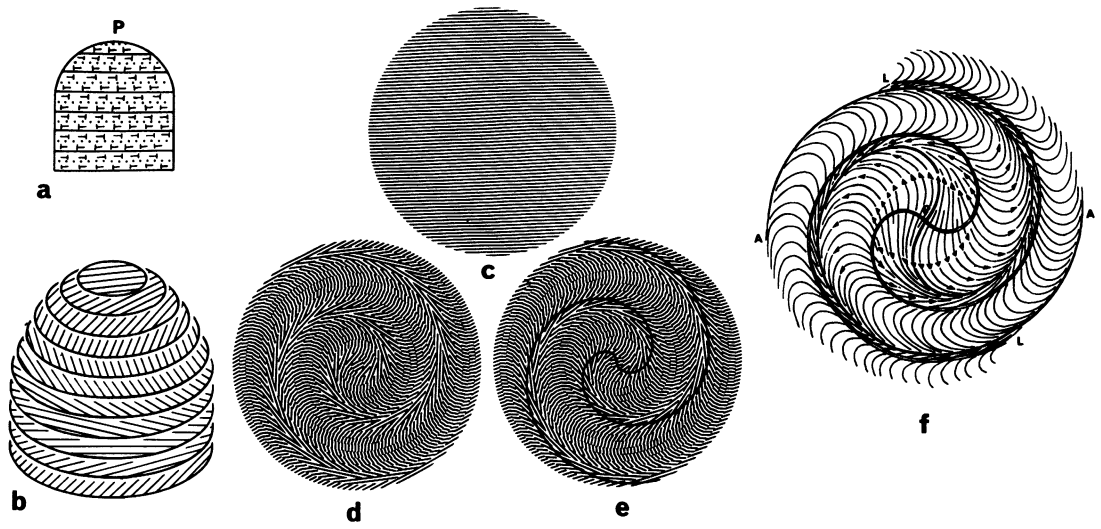

Fig. 4. — Arrangement of molecules at one pole P of a cholesteric spherulite or rodlet showing a unidirectional orientation of the cholesteric axis.
a. Meridian section of a rodlet with the nail representation (we use the term meridian section not only for spherulites showing a revolution symmetry, but also for those having a screw axis). The cholesteric structure is uniform.
b. In a perspective view the rodlet extremity can be modelized by a series of superimposed discs with the corresponding molecular orientations.
c. One of these discs is represented.
d. A set of superimposed discs is observed in top view. The disc radius regularly decreases and the molecular orientation rotates linearly. The twist is left-handed and leads to an anticlockwise double spiral.
e. The series of nested arcs form a double spiral pattern, underlined here by a curve which corresponds to directors lying parallel to the interface. This corresponds to the curve L in figure f.
f. The resulting pattern is represented with the arrowed lines convention at the interface around the pole P. The lines A and L cut at right angle in P and almost superimpose at the periphery.

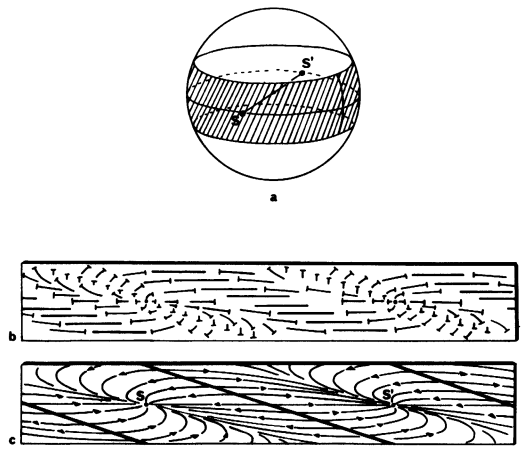

Fig. 5. — Distribution of directors in the equatorial zone of a cholesteric spherulite with a uniform distribution of the cholesteric axis. There are two diametrically opposite points S and S', where the director lies normally to the interface. The hatched equatorial zone is supposed to be sufficiently narrow to be opened at the vertical line and spread onto the plane. The nail convention is used in (b) and the arrowed lines convention is used in (c). The double lines L are oblique in this representation. SS' is a binary axis.

director lies normally to the interface. These two singular distributions of nails present an index $S = +1$, in terms of disclination theory and they correspond to a particular situation known in vector fields around points where the field is zero. In our model, spiral of arcs stop at the equator level and the concavity of arcs is changed symmetrically around these singular points which are those described in ([11], Fig. 5c).

4.1.5 *Surface distortions.* — The detailed structures, represented at the interface in figure 4f and figures 5b, c correspond to what should be observed when a non distorted cholesteric liquid crystal (a monocrystal) is cut by a spherical or an ellipsoidal interface (the long axis of revolution ellipsoid being parallel to the cholesteric axis). We think also that these drawings, namely that with force lines, are well representative of what occurs in reality. Surface tension creates distortions as quoted above, but the main effect is probably to change the obliquity of molecules with respect to the interface. Molecules are made « more parallel » or « more normal » to the interface. This would change the length of nails in the nail diagram, but this does not change appreciably their orientation within the interface and thus does not modify the topology described in these models.

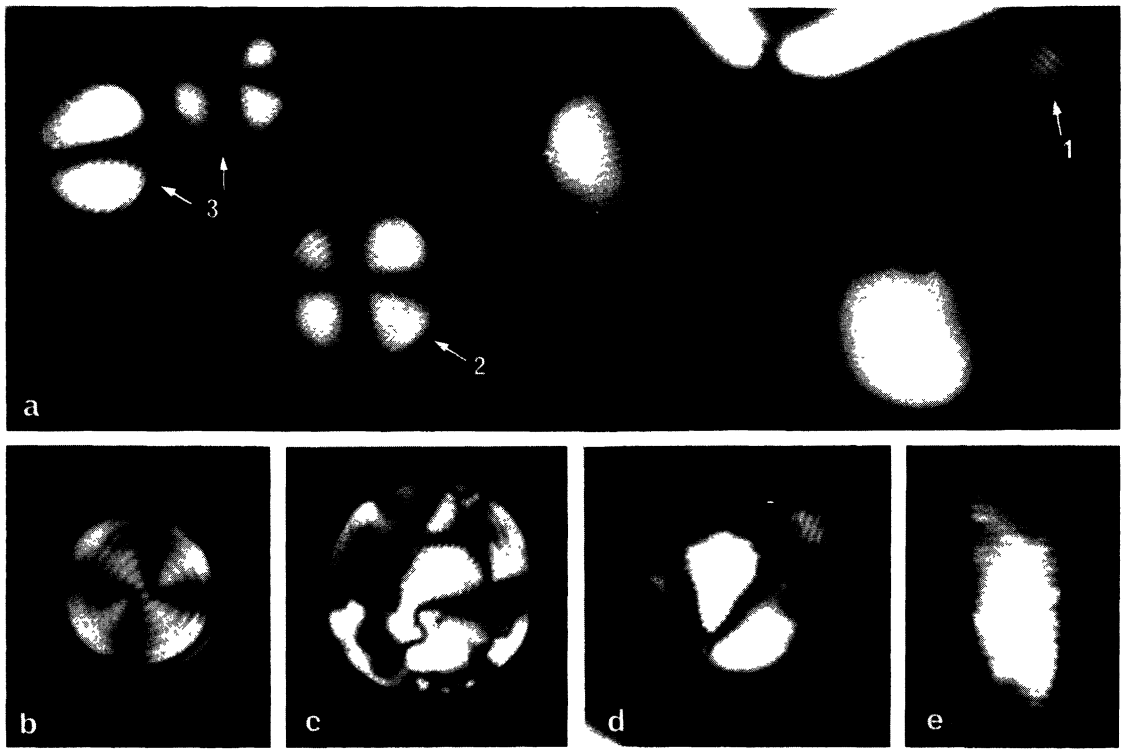

Plate III. — DNA droplets in equilibrium with the isotropic phase (a, d, e) or limited by air (b, c). Observations between crossed polars.

a. More or less spherical droplets of cholesteric phase nucleated in the isotropic phase; one observes small rodlets, with most layers normal to the interface (1). On the contrary, there is a spherulite showing layers parallel to the interface (2) and various intermediate situations (3) (× 2 800).

b, c. Droplets of cholesteric phase limited by air and the glass plates, showing a double spiralized pattern (b) or a complex texture with numerous defects (c) (b : × 2 340 ; c : × 1 530).

d. Two particular shapes of mesomorphic germs in the isotropic phase : a small bundle-shaped globule with transverse layers and a larger globule with a strong bend of layers leading to a $+ \pi$ disclination (× 2 160).

e. Rod-shaped cholesteric germ with layers normal to the long axis (× 2 340).

4.1.6 *Contrast of the interface spirals.* — Another problem concerns the origin of the contrast observed at the surface of the cholesteric spherulite in plate IVf. There is a continuous white double spiral and, in between, a dark double spiral interrupted at the apex. We think that this dark double spiral corresponds to molecules close to be perpendicular to the interface and therefore not far from being vertical and in a position of strong contrast. This means that cholesteric layers are slightly curved to remain close to perpendicular to the interface in the vicinity of the poles as represented in figure 1c. The line L follows probably the white zone, which forms a complete double spiral. If there is a tendency of molecules to lie normal to the interface, the two equatorial singular points extend and form two spiral zones running between the L lines. An obliquity of molecules, due to surface tension can make the L lines singular [15]. On the contrary, a tendancy of molecules to lie parallel to the interface suppresses the singular character of L lines, but reinforces the singular character of the two equatorial surface points. Such singular points are seen sometimes at the interface of cholesterized PAA rodlets.

4.1.7 *Morphogenesis.* — This apparently difficult morphology, with two poles P and P′ which are not singular and two equatorial singular points S and S′, is made quite natural when is considered the morphogenesis presented in figure 6. Let us suppose first the germ very small and thus, surface tension makes it necessarily spherical. If the radius is small relative to the helicoidal pitch, the spherulite resembles a nematic germ. Let us suppose now a structure without surface distortion. A nematic monocrystal is then limited by a sphere. The nail convention and the force line convention (Fig. 6a, b) show the existence of two radial singular points of strength $S = 1$; their sum is 2 and corresponds to the Euler constant of the sphere. There is also a line L running along the large circle lying normal to SS′. The structure presents a revolution axis SS′. This symmetry is broken by growth of the germ. One diameter of L is chosen

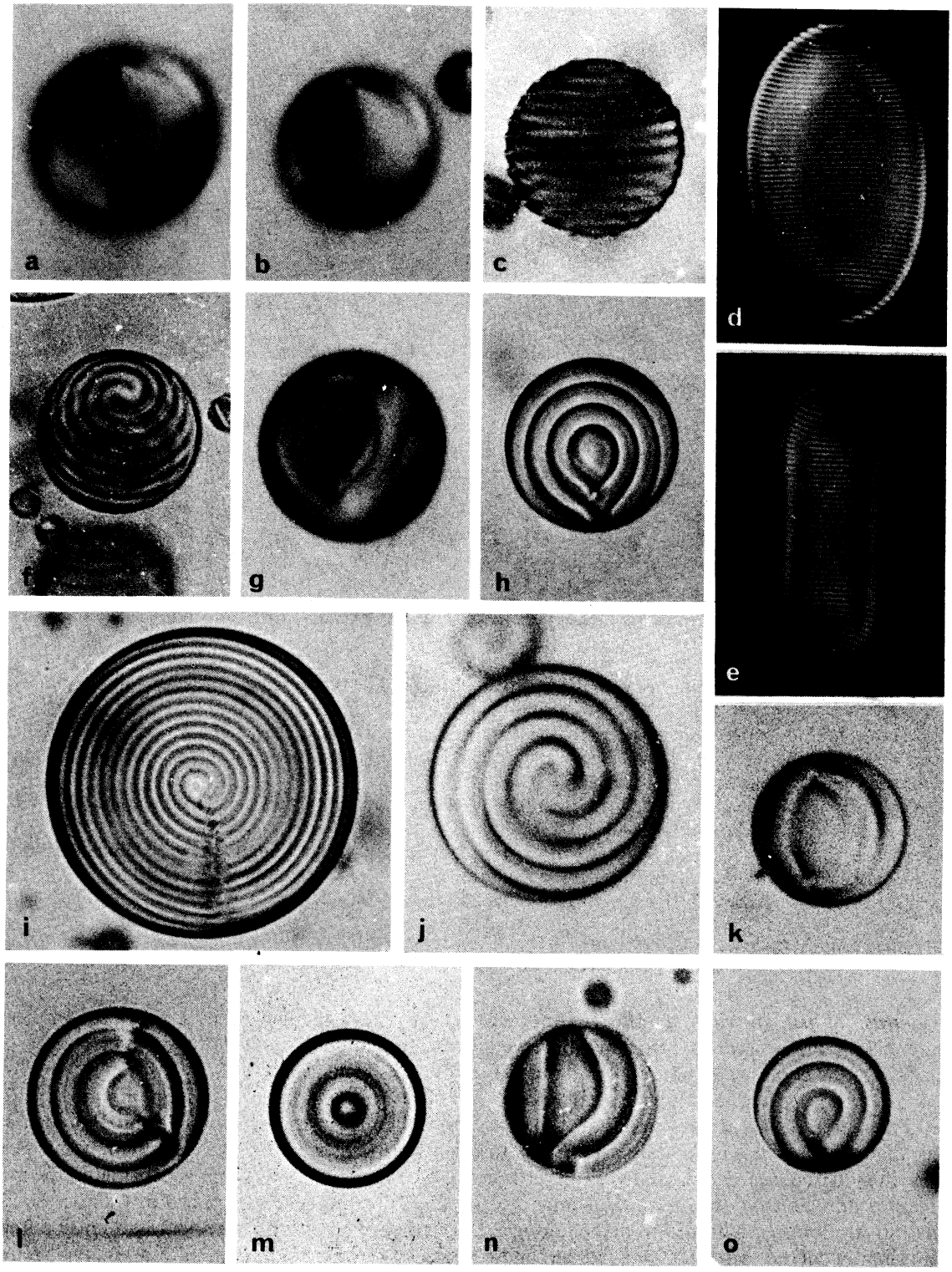

Plate IV. — Spherulites prepared with nematic MBBA or twisted MBBA (when added with cholesterol benzoate).
a. Nematic spherulite suspended in glycerol. Two point singularities are visible at the surface and are probably diametrically opposite (parallel polars, × 350).
b. A similar nematic spherulite shows two points which are certainly not diametrically opposite. Director force lines at the surface are probably very close to one of the drawings of figure 11 (parallel polars, × 560).
c. Twisted MBBA droplet in equilibrium with the isotropic phase. The cholesteric layers show a uniform orientation (white light, one polar, × 740).
d. Cholesteric droplet (MBBA + cholesterol benzoate) in equilibrium with the isotropic phase. There is an elongation which coincides with the cholesteric axis. This droplet is more or less flattened between slide and coverslip (crossed polars, × 860).

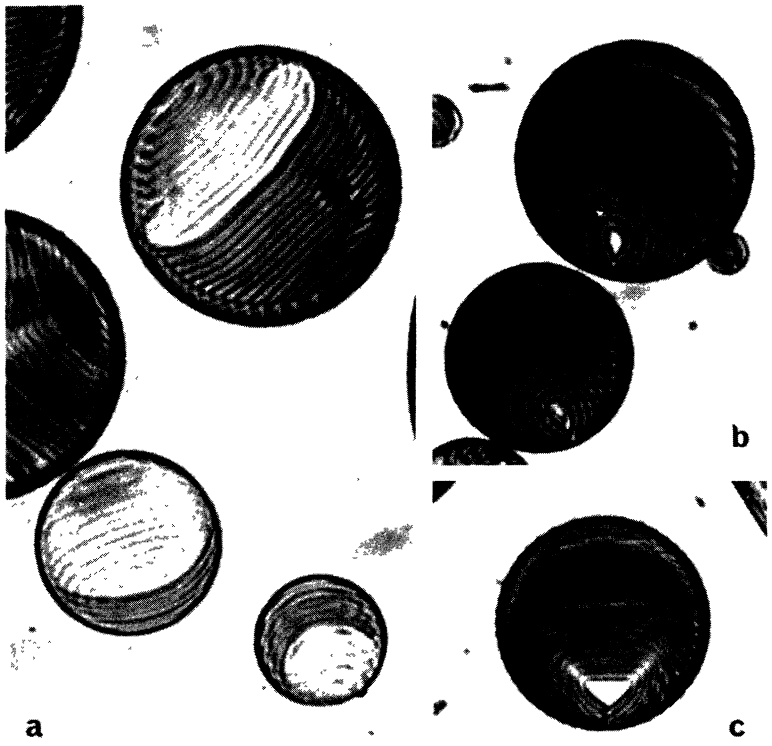

Plate V. — Spherulites of PAA with added cholesterol benzoate. Spherulites are sandwiched between slide and coverslip. There are two regions in each spherulite, a clear one where cholesteric layers are oblique (the spacing being larger) and a dark one where layers are locally vertical and contain contrasted thick threads (see 14, 15). Layers are more or less uniformly distributed in a, whereas they are curved strongly in b and, in c, a radius of disclination is formed (white light, no polars, a : × 558 ; b : × 500 ; c : × 560).

among all possible diameters of L to form the cholesteric axis. The line L ceases to be a circle. L is given by the intersection of two surfaces :

$$\begin{cases} x^2 + y^2 + z^2 = r^2 \\ y = x \tan (2\pi z/p) \end{cases}$$

which correspond to the spherulite interface and to a Riemann surface following the cholesteric pitch. The distribution of force lines is changed. These lines remain perpendicular to L in P and P′ only. The two singular points S and S′ cease to present a radial configuration. They become spiralized as shown in

e. Elliptical droplets as those of figure d can be slightly reheated and often form rodlets. Layers are strongly curved at the two extremities to remain normal to the interface (crossed polars, × 840).

f. Oblique view of the surface of a twisted MBBA spherulite in equilibrium with the isotropic phase. A continuous white and anticlockwise double spiral is visible at the interface and cuts into two parts a double dark spiral (white light, one polar, × 700).

g, o. MBBA spherulites slightly twisted by cholesterol benzoate and suspended in glycerol.

g. A single tear-drop is observed within the spherulite (parallel polars, × 740).

h. Two complete tear-drops and an open third one characterize this spherulite (white light, no polar ; × 670).

i. A spherulite with an oblique disclination radius; this picture shows a pattern intermediate between nested tear-drops (as in Fig. h) and double spirals (no polars, × 540).

j. Spherulite with its equatorial double spiral (no polars, × 810).

k. Spherulite with one or two cholesteric layers, with possibly two singular points as in figure 10d but only with a single pair of two diametrically opposite points (no polars, × 810).

l. Spherulite with a disclination curve passing through the centre (no polars, × 315).

m. Equatorial view of a spherulite showing a concentric structure (parallel polars, × 720).

n. Spherulite with a more or less distorted cylindrical structure as that shown in cross section in *m* (see Fig. 21) (no polars, × 860).

o. Spherulite with a radius of disclination. The first tear-drop is complete and the second one is in formation (no polars, × 760).

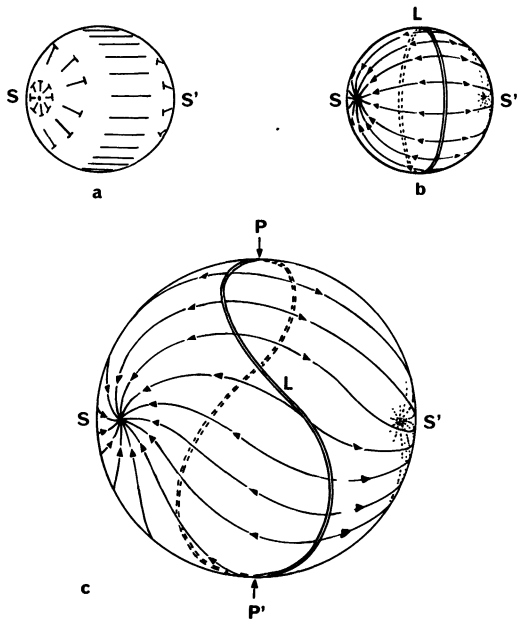

Fig. 6. — Spherulite growth. When the spherulite is very small relative to the cholesteric pitch, it does not differ from a nematic droplet with a uniform orientation of directors. a, b : Nematic initial stage of the droplet, represented with the two conventions. S and S′ are the two points where the director lies normally to the interface. When the cholesteric axis joining the two poles P, P′ is defined, the line L and the arrowed lines are progressively twisted.

figure 5. To summarize this symmetry breaking, say that, at the birth of the spherulite, the dimensions being almost zero, all diameters of L are two-fold axes. When the twist appears, one keeps only three binary axes : the PP′ and SS′ axes and accordingly the axis normal to PP′ and SS′. When the germ is growing, the line L transforms into a curve which resembles a double helix, closed at the two extremities. However, this line is not really a helix, since its angle with meridians passing through P and P′ is not constant. Similarly, one observes the formation of spiralized series of arcs and lines A joining points P, P′, S and S′ (Figs. 4f and 5c).

4.2 Spherulites with tangential orientation of cholesteric layers.

4.2.1 *Pryce and Frank model.* — Robinson presented the first description of spherulites with a radius of disclination and this was modelled by Pryce and Frank as an example of disclination of strength $S = 2$. We represented their model in figure 7a (see also [16]). They consider a sphere S and the family of circles C corresponding to the intersections of this sphere S and all planes passing through a tangent d to the sphere at point D. Now repeat the construction, using a second sphere S′, concentric to S, with a tangent d' at point D′, and the corresponding family of circles C′. D and D′ belong to a common radius R, which represents the singular radius of the spherulite.

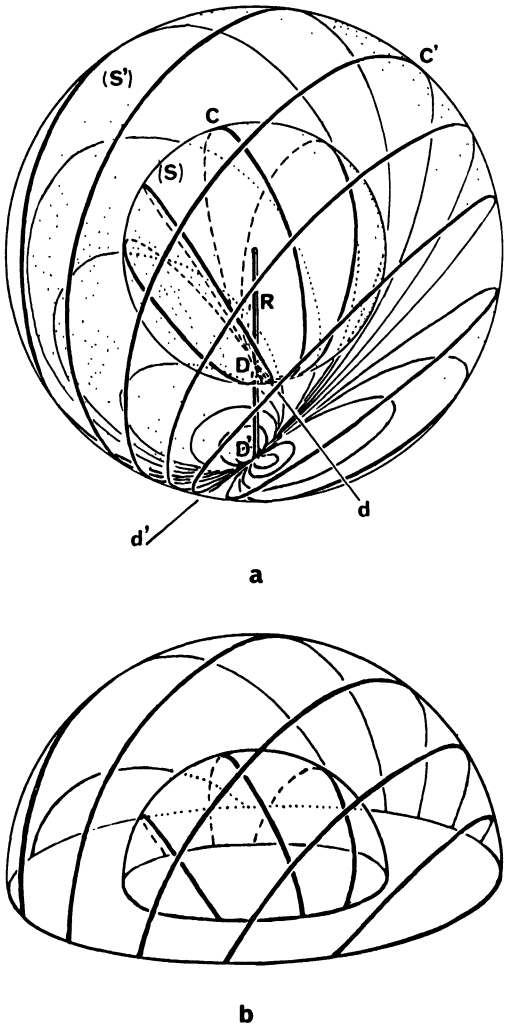

Fig. 7. — *a.* Representation of the Pryce and Frank model of spherulites with a radius of disclination. Two families of circles C and C′ drawn on two concentric spheres S and S′ are tangent respectively in D and D′ to two lines d and d′. R is the singular radius.
b. The upper part of the model, considered as a « cholesteric dome » is made of concentric hemispheres, with molecules drawing circular arcs. The rotation of molecular orientations induces the formation of a regular cholesteric layering.

Consider the radial projections of the two families of circles C and C′ onto a common concentric sphere. If an angle $\Delta\alpha$ separates d and d', each circle C cuts C′ at angle $\Delta\alpha$ along R and $-\Delta\alpha$ at any point outside of R. If the azimuth of line d rotates linearly with the radius r of the sphere S, the set of circles C form a cholesteric distribution, the twist of line d being the mirror image of the cholesteric twist.

We present in figure 7b the north hemisphere of a Robinson's spherulite modelled by Pryce and Frank. We call this structure a *cholesteric dome.*

In figure 8 we use for Robinson's spherulite the representation used in figure 4. A meridian view (a) shows two parallel sections, one in the cholesteric

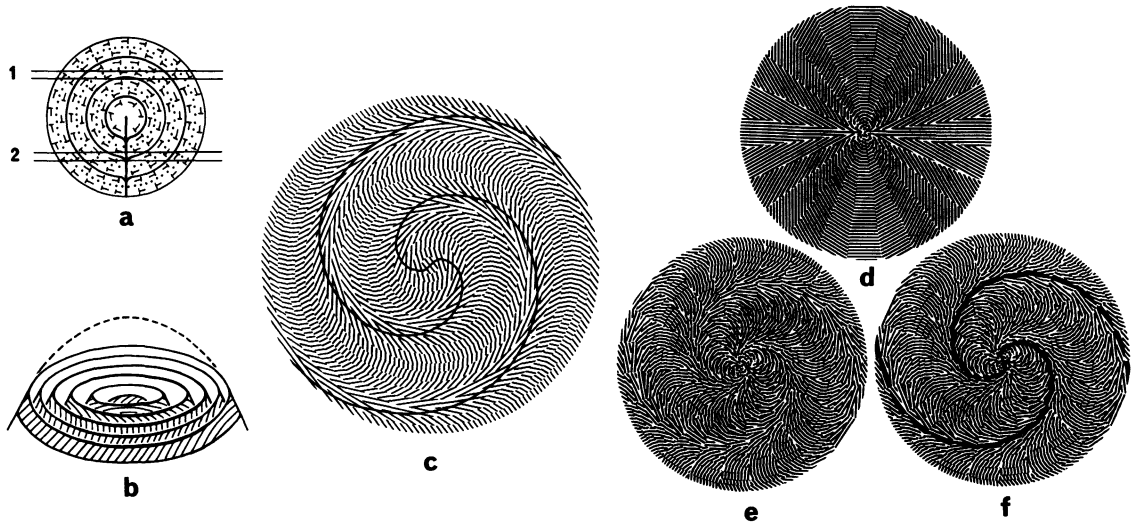

Fig. 8. — Patterns expected from the Price and Frank model.
a. Meridian view of the Price and Frank model, with the nail convention. Two types of section are considered, 1 concerns the « cholesteric dome » and 2 the disclination radius.
b. Section 1 of figure a corresponds to a slice of a series of concentric spheres, with the successive molecular orientations.
c. In projection onto the section plane, this slice shows a double spiral. A left-handed twist results here in the formation of a clockwise double spiral. This picture is the mirror image of figure 4e.
d. Representation of director orientations on a sphere around the radius *R*.
e. The section 2 of figure a corresponds to a slice of concentric spheres showing the pattern represented in d. Each sphere gives here a narrow circular ribbon. Each ribbon is regularly rotated relative to the preceding one. The series of nested arcs form a double spiral which is also clockwise. The arcs show a centrifugal concavity in figure c, whereas this concavity is centripetal in e and f.
f. The asymptotic line A is underlined.

dome (1) and the other one across the singular radius (2). The thin section (1) is formed by a central cap and by concentric ribbons which correspond to successive orientations of the cholesteric structure (b). A projection onto the section plane gives the pattern represented in (c) with its double spiral whose chirality is opposite to that of figure 4e. A way to obtain the structure of section (2) is to follow the procedure described in figure 4. We start from the pattern observed in the bottom of one of the spheres in figure 7. This system is represented in figure 8d. Section (2) is made of concentric ribbons as section (1). Figure 8d can therefore be divided into concentric ribbons, each one being rotated by a small angle relative to the preceding one. This leads to figure 8e, which presents a double spiral of nested arcs. The limits of arcs are underlined in figure 8f. It must be noted that arcs show a concavity opposite to that observed in figure 8c.

In figure 9 are applied the two conventions, nails or arrowed lines, to the pictures of figure 8. There are three section planes (1, 2, 3) lying normally to the radius. (1) cuts the cholesteric dome, (2) is the equator plane and (3) cuts normally the disclination radius. For each section (b_1, b_2, or b_3), the director orientation is indicated along one circle only, with the nail convention. Finally, the patterns observed in planes (1), (2) and (3) are represented in c_1, c_2 and c_3, with the arrowed line convention. This figure is different from figure 8, since it indicates the molecular obliquities shown by the arrows and the relative positions of spirals A and L. One must note that the spiral observed in figure $9c_1$ is similar to that of figure 4f, but of opposite chirality, though the twist is left handed in both situations. Passing from plane 1 to plane 3 leads to an inversion of arc concavities, whereas the orientation of spirals is unchanged. The equator plane shows an intermediate situation, without arcs, layers being vertical.

4.1.2 *Related models.* — We only gave here a more detailed presentation of the Pryce and Frank model. We shall transform it later into a continuous model. Let us now just consider some other spherulitic configurations which are linked very naturally to the Pryce and Frank model.

Ribonucleic acid (RNA, probably ribosomal RNA, see Spencer *et al.* [17]; Spencer and Poole, [18]) may form spherulites showing a diameter instead of a radius of disclination. We also mentioned the existence of such spherulites, with a concentric structure in xanthan (plate II, e). A possible model drawing its inspiration from the Pryce and Frank interpretation, is represented in figure 10. A meridian section is drawn in figure 10a. This corresponds to concentric spheres (1), (2), (3) ..., with force lines following meri-

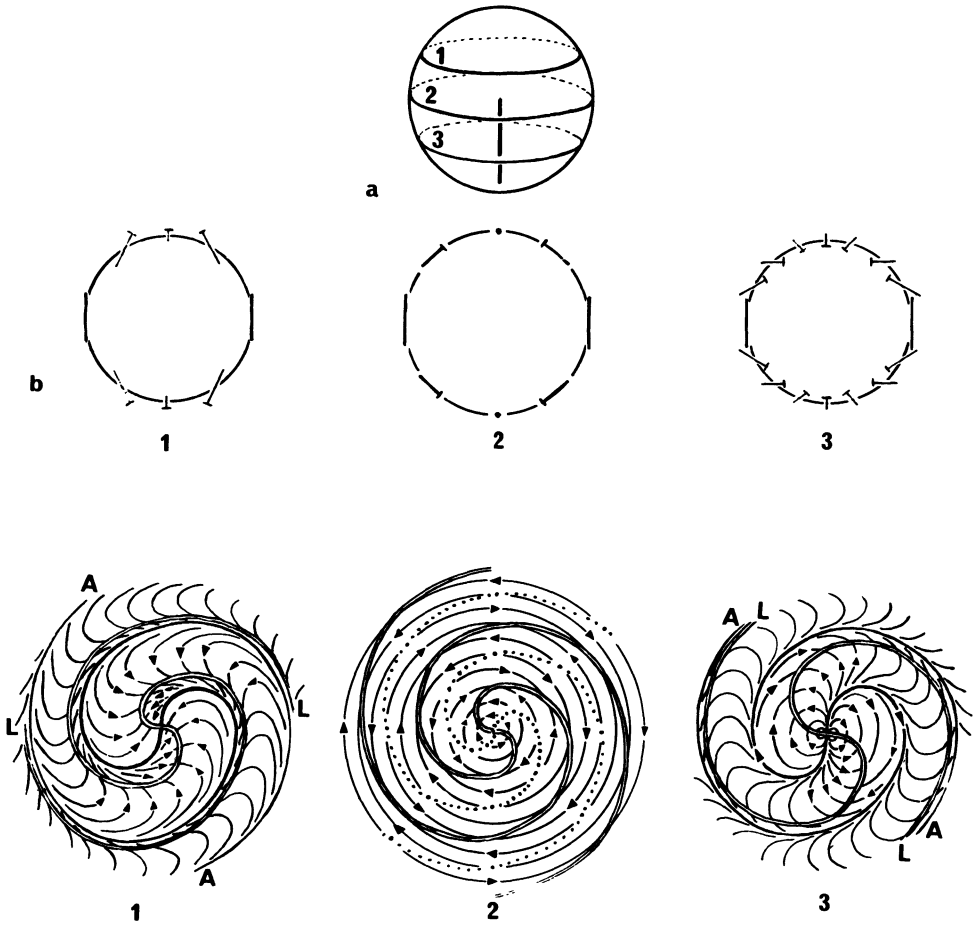

Fig. 9. — **a.** Three section planes of a spherulite showing a singular radius.
1 : Horizontal section of the « cholesteric dome ».
2 : Equatorial section.
3 : Horizontal section of the singular radius.
b. Arrangement of directors (represented by nails) along the sections of one sphere only by plane 1, 2 and 3 respectively.
c. From patterns of figure b, is easily found the complete structure of sections 1, 2 and 3 in the nail convention and then with the arrowed lines convention. Lines A and L are represented and their relative position is different between 1 and 3.

dians (a_1 and b_1), helices (a_2 and b_2), parallels (a_3 and b_3), helices with opposite chirality, meridians, etc. On each sphere appear two singular points (S and S'), surrounded by a radial configuration (b_1) or a spiral one (b_2) or a series of concentric circles (b_3). The superposition of these configurations around the singular diameter is shown in figure 10c. The spherulite shows a revolution symmetry about its disclination diameter. Similar models were already presented by Lagerwall and Stebler [19]. This disclination diameter can be replaced by a series of disclination points as is shown in figure 10d, e. This transformation does not alter the revolution symmetry.

In our preparations of twisted MBBA droplets, floating in glycerol, we encountered spherulites showing a singular curved disclination line (Pl. IV, l). Such a situation might correspond to the bending of a singular diameter. This does not change the whole topology described in figure 10. This disposition of force lines on successive concentric spheres is represented in figures 11a, b, c. If singular points become closer and closer and finally join, each figure 11a, 11b, 11c, leads to figure 11d which corresponds to the Pryce and Frank configuration. This process shows how to pass continuously from spherulites with a singular diameter to those of Robinson, with a singular radius.

4.2.3 *Continuous model of the singular radius.*

• Contrast of vertical directors and thick threads. — This new conception originates from the analysis, presented some years ago, of close thick threads often observed in cholesteric liquids. Some of these threads present a characteristic tear-drop shape [15]. One must first recall that thick threads, easily observed in slightly twisted nematics, correspond to the locus of directors parallel to the observation direction (the microscope axis). If the coordinate frame is chosen

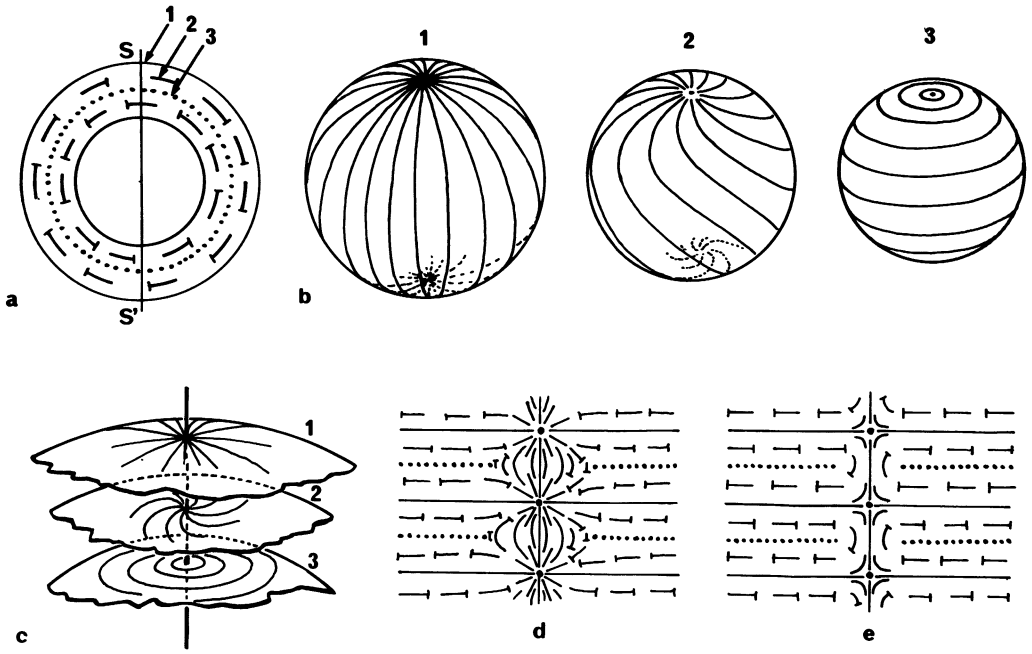

Fig. 10. — Models in the Price and Frank style of spherulites with a disclination diameter.
a. Meridian section with the singular diameter SS' represented with the nail convention; three different concentric spheres 1, 2, 3 are considered.
b. Director force lines are represented on spheres 1, 2, 3 and form either meridians, spherical helices or parallels. This is a disclination $S = 1$.
c. Three successive layers 1, 2, 3 are represented around the disclination.
d, e. The disclination line can be transformed into a series of radial singular points (+ I) (d) or (− I) (e) represented here in meridian view. Note that the twist is positive about the revolution axis in d whereas it is negative in e. Since the cholesteric twist is left-handed, the structure e requires less energy than d. Both situations are topologically stable, but d is quite unlikely.

with its axis Oz parallel to the microscope tube, the locus of vertical directors corresponds to lines which are the intersection of the two surfaces :

$$n_x(x, y, z) = 0 \quad \text{and} \quad n_y(x, y, z) = 0$$

n_x and n_y being the director components along x and y.

• Threads with the shape of simple or nested tear-drops. — The origin of threads folded back into tears-drops is explained in figure 12a, redrawn after our previous work [15]. Cholesteric layers are slightly folded in a plane 1. From such folds, two edge-dislocations can appear in the cholesteric liquid (plane 2). Each edge-dislocation is composed of two disclinations : $\lambda^{-\pi}$ and $\lambda^{+\pi}$.

The line which is almost half-way between these two λ disclinations, corresponds to the locus of vertical directors and therefore is observed as a thick thread. The situation described in plane 3, 5 is similar to that drawn in plane 2.

Now, let us look at the three half-planes 3, 4 and 5. The structure is the same in each of them, but the difference is that they lie at three different levels, according to the different orientations. The cholesteric liquid is supposed to be left-handed as shown in planes 1, 2 and 4. The structure represented in plane 4 is deduced from that in 3 by a helicoidal displacement (axis : intersection of 3 and 4; angle : $+ \pi/2$; translation : $p/4$, p being the cholesteric pitch). One passes from 4 to 5 by the same helicoidal displacement. This helicoidal displacement is due to the helicoidal structure of the cholesteric liquid itself : the level of an edge dislocation changes by $\Delta l = \Delta\alpha \frac{p}{2\pi}$, when this dislocation shows a horizontal angular variation of $\Delta\alpha$ [16].

Between plane 3 and 5, $\Delta l = p/2$ and $\Delta\alpha = \pi$. It is shown in figure 12a that a closed thick thread presents a cusp which annihilates the $p/2$ gap created by a half loop. The aspect of such tear-drops is presented in figure 12b ([3a]).

The pattern drawn in plane 2 of figure 12a can be considered as the beginning of a spiralized structure.

([3a]) A way to create these tear-drop in slightly twisted nematic liquids (MBBA + a small quantity of cholesterol benzoate, for instance) is to blow on a free surface drop of this mixture stretched on a glass slide. Very numerous tear-drop form and disappear when the blowing ceases : this shows how this structure is created or relaxed continuously.

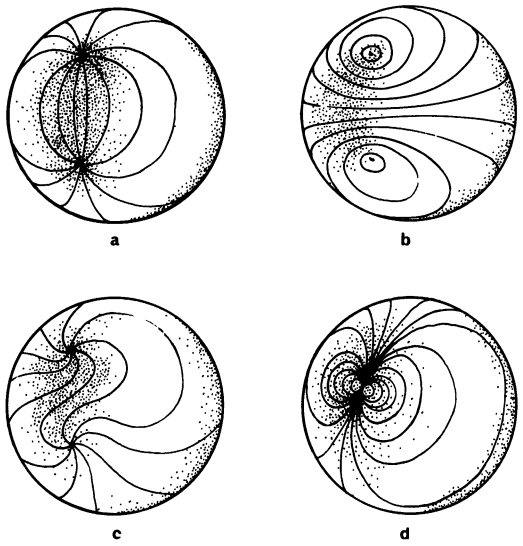

Fig. 11. — Certain spherulites show a disclination arc instead of a diameter, and spheres 1, 2 and 3 of figure 10a must be transformed. Consider a sphere and, on this sphere, the set of circles passing through two given points, which are not necessarily diametrically opposite. An inversion centered on one of these points transforms the sphere into a plane and those circles into a set of concurrent straight lines. In this plane, the curves which cut these straight lines at a given angle are either logarithmic spirals or concentric circles. Coming back to the spheric representation, a cholesteric layering can be built, starting from a sphere with two poles, which are not diametrically opposite, since such mappings are conformal.

a. Set of circles passing through two any points of the sphere.

b. Family of circles cutting normally those of figure a.

c. Spiralized patterns obtained by inversion from a family of logarithmic spiral in a plane.

d. When the two poles fuse, any of figure a, b and c tend to the pattern considered in Price and Frank model.

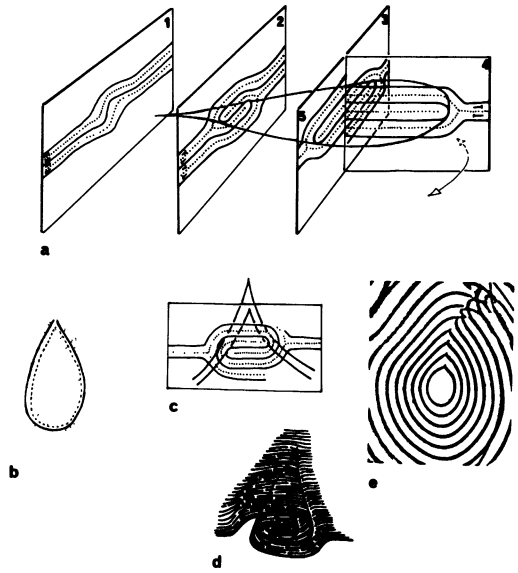

Fig. 12. — Model of a thread folded back into a tear.

a. In a plane 1, the cholesteric layer is slightly distorted and a double fold appears in plane 2. This double fold can be considered as a set of two edge-dislocations, which differ by a vertical distance of $p/2$, the half-helical pitch. In plane 3, 4 and 5, this edge-dislocation forms a helical arc which follows the cholesteric helicity : the rotation angle is $-\pi$ and the vertical displacement is $p/2$, since the cholesteric liquid is supposed to be left-handed. This vertical displacement compensates the vertical shift due to the double fold.

b. Aspect of such a « tear-drop » (redrawn after a micrograph in [15].

c. Origin of « nested tear-drops ». A double fold can be progressively spiralized and leads to a system of threads forming nested cusps.

d. The surface where directors are parallel to the plane represented in c is drawn in perspective.

e. Set of nested tears obtained in MBBA doped with a very small crystal of cholesterol benzoate (redrawn after a micrograph in [15]).

This process is continued in figure 12c. In this case, the locus of vertical directors forms two nested cusps. The surface corresponding to directors parallel to the section plane can be isolated and this corresponds to the spiralized sheet represented in figure 12d. This shows clearly the origin of cusps. The two edge-dislocations in figure 12c have Burgers vectors equal to $2p$. However their mean levels differ by $p/2$ and the helicoidal displacement described in planes 3, 4, 5 of figure 12a also applies to this case. We get therefore two concentric tear-drops. This spiralization process can be pursued and this gives a set of concentric tears with aligned cusps, as shown in figure 12e, reproduced from a previously published micrograph [15] ([3b]).

To facilitate the visualization of these structures, we represented a single tear-drop in figure 13. We limit the drawing to the locus of vertical directors which forms the tear-drop itself and to the surfaces which correspond to directors normal to tangent at the cusp point in horizontal projection and also the ribbons formed by the force lines of directors passing through the thread in the region of the half-loop.

When a crystal is just dissolved, there is a maximum of twist, surrounded by regions which are less twisted. Concentric tears are formed and separated by intervals of increasing size at the periphery (Fig. 12*e*). Similar sets of nested tears were also observed in PBLG and in Xanthan spherulites as described above (Pl. I and II); they are well resolved in MBBA spherulites suspended in glycerol (Pl. IV*h*). We also noticed in these preparations a spherulite with a unique tear-drop (Pl. IV*g*).

([3b]) The way to get such pictures is easy. Between two rubbed glasses, one introduces a nematic liquid crystal, MBBA for instance, in which are added some very small cholesterol benzoate crystals, working as a twisting agent.

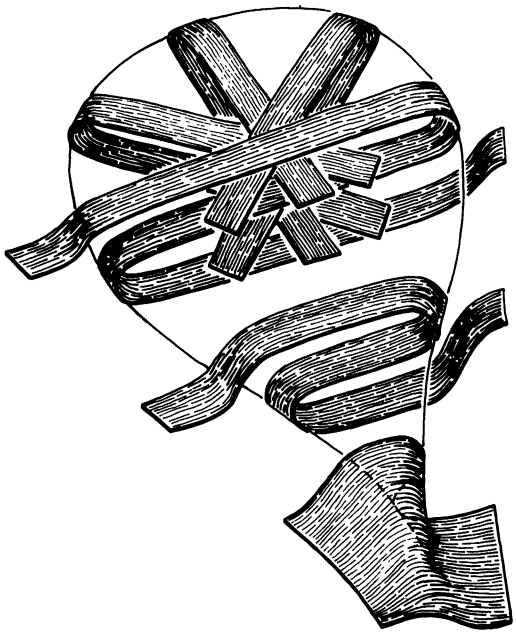

Fig. 13. — Model of the tear-drop. The thick thread in the form of a tear-drop corresponds to the locus of vertical directors (parallel to the microscope axis). The surfaces represented are those formed by the force lines of directors passing through the thread. The cusp corresponds to the birth of a double fold. The second ribbon shows a double fold which corresponds to a set of two edge-dislocations in the cholesteric structure. In the circular part of the tear, there is a set of ribbons which transform from one to another by a series of screw displacements $\left(-\frac{\pi}{4}, +\frac{p}{8}\right)$. (Each ribbon is built on a short thread segment supposed to be straight, in order to avoid forming a Riemann surface in the centre of the tear-drop).

The twist was supposed to be left-handed, as in all materials examined in this work. We hope, by this drawing, to give a complete and global perception of this remarkable continuous structure formed by tear-drops in cholesteric liquids.

• Global model of Robinson's spherulites. — Another picture leads to a better visulization of the global configuration of the spherulite. Let us consider two hemispheres, separated by the equator plane (Figs. 14a, g). In each hemisphere will be represented two main orientations of molecules, separated by a right angle. In the upper hemisphere, the nested domes are again found, as in figure 7b. In the lower hemisphere there is a spiralized sheet as in figure 12 and the added layers at right angles. This structure differs from the lower part of the Pryce and Frank model. The structures observed on both parts of the equator plane are different (circles *versus* spirals), but slight angular deviations suffice to transform one to the other. This passage is illustrated in figures 14b-f, with the nail convention. The figures 14b and 14f correspond respectively to the upper and lower hemispheres in the equator plane. The difference is that in b, nails are aligned along concentric circles, whereas in f, they are slightly oblique, relative to the same circles, and they form spirals. In figures 14c and e, we have isolated a single circle from figure b and f respectively. It is easy to align molecules of figure 1 along the circle and to obtain figure d. It appears that figures c and d are symmetrical, but correspond to the same structure seen from opposite sides as in figures a and g.

The centre of the spherulite is not singular. Figures 14a and b could lead one to suppose a discontinuity when the radius of upper hemisphere shells tends to zero. Actually, we did not represent such central shells. There is a continuous passage of molecular orientations from one hemisphere to the other in the central region and this is described in figure 15. When domes become smaller than the helical pitch, the hemispherical shape is lost and shells transform progressively into discs. The passage from above to below the centre is represented in four successive horizontal planes in figure 15 indicating the continuity of molecular orientations at the centre. This continuity was already obvious from the above study of nested tears.

To end the exploration inside this spherulite, we think useful to show an enlarged view of the radius itself and its helicoidal symmetry. We consider here the surface which is the locus of directors lying normal to the radius. The directors lie practically tangent to this surface. This surface is generated by a horizontal double spiral whose centre describes a vertical straight line and whose orientation rotates linearly with the vertical coordinate (Fig. 16). This leads to the formation of nested cusps. This surface separates two regions, in the form of two grooves in which are nested two $\lambda^{+2\pi}$ disclinations, as shown on the cross section of the radius (Figs. 17a, a'). A meridian section is also represented in figures 17b, b' and reveals the absence of singular points. The passage from the discontinuous disclination of Pryce and Frank to a continuous one is presented in figure 18. The cross section of the disclination $S = +2$ is replaced by a set of two $S = +1$ with a continuous core.

5. Discussion.

5.1 MOLECULAR ORIENTATIONS AT THE INTERFACE. — We already indicated that germ configurations are related to molecular orientation at the interface. Parallel orientations lead to concentric spherulites, whereas normal orientations favour a uniform distribution of layers as in many spherulites and rodlets. The question remains why molecules follow preferentially one of these two possible orientations. Until recently, behaviour of molecules at the interface was presumed to be related to length of molecules themselves. Indeed, concentric spherulites were described only with long molecules of PBLG by Robinson, while rodlets with a uniform orientation of layers were observed with small molecules in

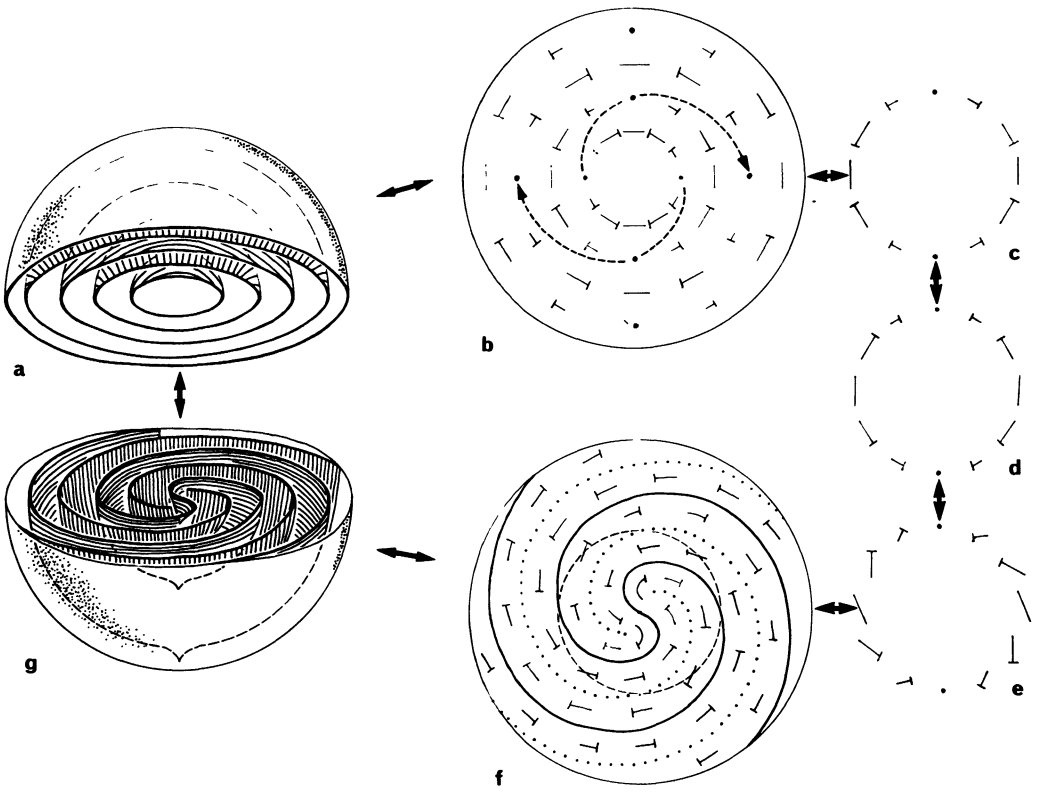

Fig. 14. — Exploded spherulite.
a. The « cholesteric dome ».
b. The nail convention applied to the equatorial plane along the cholesteric dome and its clockwise spirals.
c. Nail distribution in b along the equator of a single sphere.
d. Nail distribution of c viewed from the opposite side.
e. This nail distribution is obtained from a continuous transformation of that shown in d, and corresponds to that drawn in the following figure.
f. Equatorial structure, with the nail convention applied to the hemisphere with the singular radius.
g. The lower hemisphere with its continuous cholesteric structure, which is detailed in figure 16 and 17.

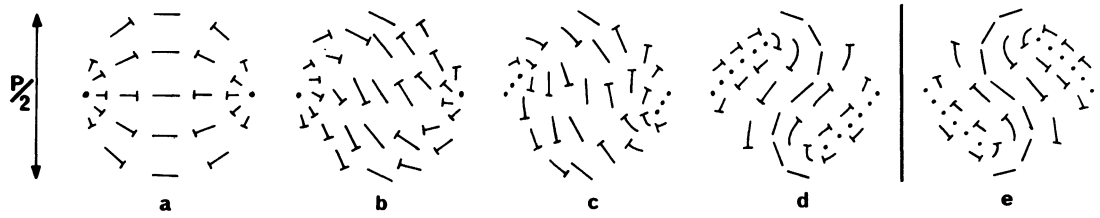

Fig. 15. — Structure of the central region of the spherulite, in four successive horizontal planes : (a) slightly in the upper hemisphere, (b) in the equator, (c, d) in the lower hemisphere. a, b, c, d are observed from below as in figure 14b and e viewed from upon as in figure 14f.

general. Our study shows that all situations are possible and that there is no general rule. We know examples of parallel anchoring of small molecules (twisted MBBA in glycerol) and of very long molecules such as polymers (PBLG, xanthan and DNA). In the same way, germs with uniformly distributed layers are obtained with small molecules (twisted MBBA when molecules are suspended in their isotropic phase) as well as with polymers (DNA). Molecules which can form the two types of rodlets also present intermediate types (PAA, DNA).

Two other characters must be taken into consideration : *the size of rodlets* and *the isotropic phase in which they are suspended.* Indeed, twisted PAA spherulites show first a uniform distribution of cholesteric layers and, after growth, present a strong tendency to concentric arrangement. Besides, twisted MBBA forms concentric spherulites in glycerol and rodlets

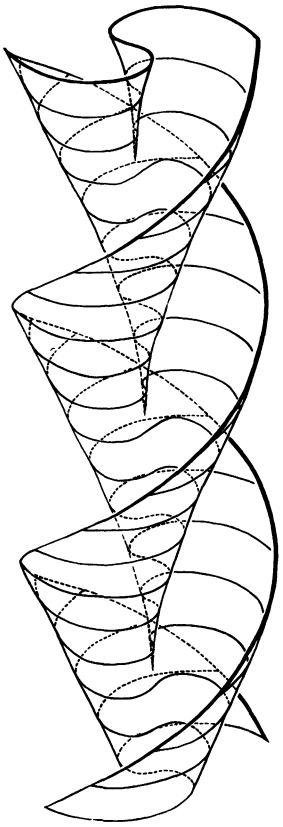

Fig. 16. — Fundamental surface modelling the architecture of the radius of disclination. This surface is the locus of molecules lying normal to the radius, in its vicinity. This surface is generated by the screw displacement of a double spiral. The series of nested cusps corresponds to the locus of directors parallel to the observation axis (or microscope axis).

with uniform orientations of layers in the isotropic phase. However, even in similar conditions a polymorphism may appear : DNA rodlets with uniform orientation of layers coexist with droplets showing a concentric structure and with rodlets of intermediate type. The polymers used are not monodisperse and the *heterogeneity in the molecular lengths* should be responsible for additional variations.

In the case of twisted PAA spherulites, very small germs present a constant orientation of layers and there are two identical poles P and P'. One of these poles will be chosen for the invagination which occurs later in growth. This is a breaking of symmetry. This supposes also strong variations in angular boundary conditions, which are possibly related to proportions of components and impurities in the mesophase.

5.2 OTHER EXAMPLES OF DISCLINATIONS WITH CONTINUOUS CORE. — The main patterns of disclinations supposed to exist in classical liquid crystals are found in the works of Friedel and Grandjean [20], Grandjean [21], Oseen [22], Frank [23] and Robinson [4]. Continuous disclination cores were first presented in papers due to Kléman and Friedel [14], Bouligand and Kléman [16]. The continuity of the core of a $S = +1$, for a nematic observed in a capillary tube treated for homeotropic conditions, was predicted by Cladis and Kléman and subsequently observed by Williams *et al.* [24]. The continuity of a $S = -1$ was shown by Meyer [25]. The continuous model of $S = 2$ is presented in a general study of threads observed in Grandjean-Cano wedges [15], where the resemblance with the singular radius of Robinson's spherulites was also pointed out. However, we had not observed the spherulites at that time. The nested tears were also described by Williams and Bouligand [26] when a cholesteric liquid is introduced in a capillary tube, in homeotropic conditions. Cladis studied the transition from a smectic A to a nematic phase [27] or to a cholesteric phase [28], in a capillary tube with homeotropic conditions. A planar and discontinuous $S = +1$ present along the capillary axis transforms into a continuous core in the nematic phase. In the cholesteric case, Cladis supposed that the $S = +1$ gives rise to two $S = -\frac{1}{2}$ and to a $S = +2$ decomposed into two continuous $S = +1$. The pictures are remarkable, but there are still questions to solve in this situation. The patterns are very different from the series of nested cusps, for a disclination $S = +2$, in its continuous form, as were observed by Williams and Bouligand [26] in the case of a cholesteric liquid filling a capillary tube in homeotropic conditions. More studies seem therefore to be necessary to complete the observations due to Cladis *et al.* [28].

5.3 COMPOSITE SPHERULITES AND GENESIS OF TEXTURES. — Several micrographs show that spherulites can fuse to make larger drops. The main defects arising from the coalescence are $-\pi$ disclinations, which are easily observed between crossed circular polarizers. The core appears to be black in general and this indicates that preferred disclinations are $\lambda^{-\pi}$ (Pl. I, d, i, j; Pl. II, f). This analysis is easy for PBLG and xanthan but is more difficult for DNA cholesteric phases (Pl. III, c). However, in this material, dislocations and disclinations were analysed in great detail by Livolant [12]. One finds $\lambda^{-\pi}$ disclinations only. The coalescence of cholesteric droplets was also studied in the case of MBBA with either Canada balsam or cholesterol benzoate [29]. Such germs which show a uniform orientation of the cholesteric axis, fuse with the formation of a $-\pi$ disclination if their cholesteric axes make a sufficient angle, and without disclination, when they are not far from being parallel. When a disclination forms, it happens very often that it joins the interface and disappears. Series of alternating $+\pi$ and $-\pi$ disclinations form when large drops fuse. These processes of coalescence determine almost completely the textures which grow from isotropic phases. In phases which result from the junction of spherulites with a concentric texture,

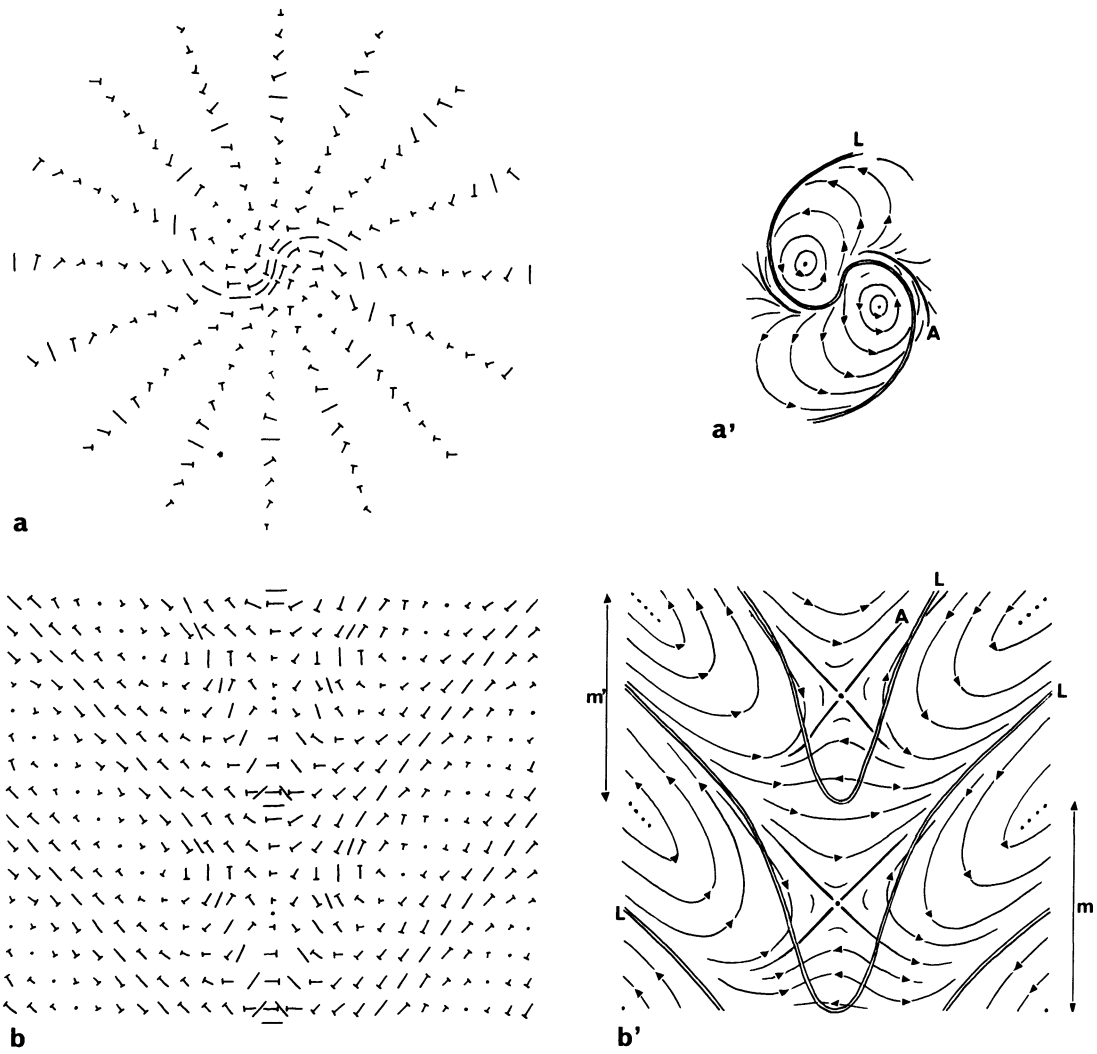

Fig. 17. — Cross section (a, a') and meridian section (b, b') of the disclination radius with the nail and the arrowed lines conventions. Lines A and L are indicated. m and m' are vertical periods and m is transformed into m' by a right-handed screw displacement.

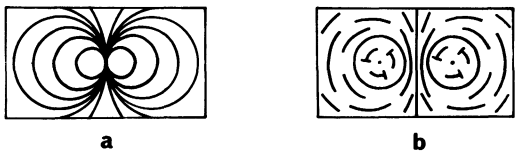

Fig. 18. — The discontinuous model due to Price and Frank (a) is very simply transformed into a continuous one (b).

the original spherulites are often recognized, with their initial double spiral or their singular radii (see Pl. I, k, l and also [3]). One must note that there are two possible origins for a $-\pi$ disclination in this case : two spherulites coalescence and new layers form or three germs coalesce. These two different processes are observed in plate I, l.

5.4 Occurrence of twisted spherulites.

5.4.1 *Frequent and rare spherulites.* — Robinson's spherulites with a disclination radius, spheric or elongated germs with a uniform orientation are very frequent. The other forms we studied seem to be less frequent or rare. Disclination diameters described in RNA by Spencer *et al.* [17] are rarely observed in xanthan and we spent a very long time only to find some unremarkable examples in MBBA. The reason could be, as pointed out by Stein *et al.* [30] that the $S = 2$ configuration on the sphere (Fig. 11d) corresponds to an energetic minimum relative to the other situations sketched in figures 10a, b and figures 11a, b, c.

5.4.2 *Polymer crystals.* — Banded spherulites, with concentric layers were observed in many crystalline polymers such as polytrimethylene glutarate and

Keller [5, 31, 32] studied many examples of such textures. Keller and Point established how the biaxial index ellipsoid shows a helicoidal arrangement along the radii (Ref. in [5]). The texture is polycrystalline and the slow axis of the ellipsoid follows a cholesteric geometry. There is a difficult problem underlying these textures : the polymer is regularly folded and forms parallel lamellae separated by intervals containing disordered chains. The polymer scans up and down the thickness of lamellae a great number of times and lies mainly normal to the plane of lamellae, sometimes leaving a lamella, to fill the interspace. These lamellae form ribbons extending radially from the spherulite centre. These ribbons make a regular twist and form a cholesteric texture [33] (Fig. 19). Topologically, it is impossible to arrange in such a way a set of ribbons and a very high density of defects is expected. It appears therefore that observations of sophisticated defects such as disclination radii are to be excluded and actually there are no reports of disclination lines in these studies.

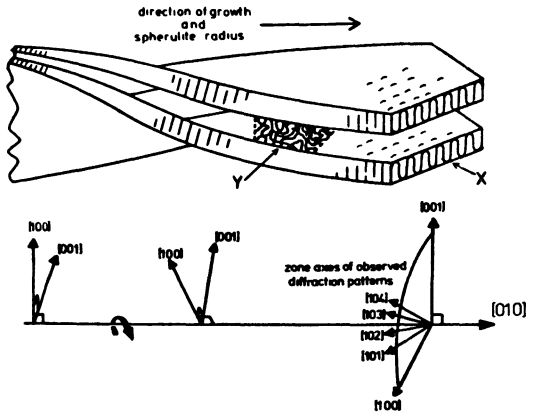

Fig. 19. — Schematic representation of the twisted lamellae model of a polyethylene spherulite, showing the regularly folded (X) and interlamellar (Y) chains, and the variation in crystal axis orientations with positions along a spherulite radius (from [33]).

5.4.3 *Other examples of banded spherulites.* — Keller's articles are also well documented sources of bibliography and remarkable older studies are reviewed. It is recalled that Michel-Lévy and Munier-Chalmas [34] described in chalcedony, a biaxial variety of silica, spherulites made of radial needles. The fast axis is aligned along the needle axis, whereas the slow and the intermediate axes rotate along this long axis as in a cholesteric structure. The different needles are in phase and form banded spherulites in the polarizing microscope. This model was later followed by Wallerant [35], Gaubert [36] and Bernauer [37] who studied various inorganic and organic substances forming similar banded spherulites.

5.4.4 *Cholesteric spherulites and rodlets in living systems.* — Lison [38] noted the existence of mesomorphic inclusions in cells and tissues, but he remarked with reason that it should be ascertained if these droplets are still true mesophases at body temperature. These inclusions are supposed to contain mainly cholesterol derivatives. Such liquid crystalline inclusions were studied in endocrine tissues such as *adrenal cortex* and *corpus luteum* [39]. These secretion droplets are possibly isotropic at 37 °C. At room temperature they seem to be nematic, with often a slight twist. Similar mesomorphic droplets were observed in the walls of arteriosclerotic blood vessels [39]. Beautiful Robinson's spherulites are recognizable in micrographs of oothecal secretions of certain praying mantis [40-42]. The eggs of certain parasitic worms and cysts of protozoa are limited by a very hard shell which is a hardened cholesteric structure with concentric layers [43-44]. This needs the presence of defects, possibly a disclination radius, but there is still no evidence of it.

Certain polysaccharides form cholesteric inclusions in the cytoplasm of marine worms [45] and show a relatively uniform orientation of layers. In larval hemocytes of the silkworm, large cholesteric spherulites with a concentric arrangement of layers are observed. They are made of fibrous proteins [46]. Dinoflagellate chromosomes are cholesteric aggregations of DNA, devoid of histones, but probably associated to other proteins. These chromosomes are more or less spherical in Zooxanthellae [47] and elongated in *Prorocentrum* [48]. Other spherical drops of cholesteric DNA are found in certain bacteria [49, 50] and in the kinetoplast of Bodo [51]. Certain bacterial nucleoids present a toroidal arrangement as that drawn in figure 20 (Thomas, personnal communication). A topologically similar structure is observed in other bacterial nucleoids which are no more rodlets but real torus [52]. The configuration described in figure 20 was also observed in small cholesteric germs of collagen growing *in vitro* from a concentrated solution [53] and in spherulites made of fibrous proteins in proteoplasts in the phloem of Abietacae [54]. Some intermediate spherulites were found by Gourret [54, 55] in cell vacuoles of root nodules of the legume *Vicia*. They show a cylindrical and coaxial

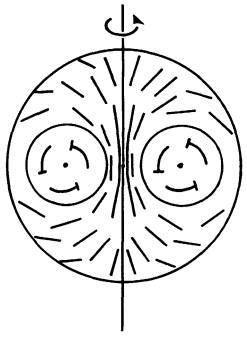

Fig. 20. — Toroidal spherulite. The nail convention is applied in a meridian plane. There is no discontinuities of molecular orientations.

arrangement of cholesteric layers about a $\lambda^{+2\pi}$ disclination (Fig. 21). This corresponds to the configuration drawn in figure 1i and 1 in cross and longitudinal section. Besides, bacterial viruses can form spherulites and « deformed spherulites » when a concentrated gel is stored in sealed quartz capillaries. A radial line of disclination is thus observed [56].

5.5 SURFACE DEFECTS. — A brief review of our models shows first that all cholesteric germs (concentric structures with a radius of disclination, or with uniform orientation of the twist axis) never present any discontinuity in the bulk and secondly that all these textures are generated continuously from an initial monocrystalline nematic spherulite. There is a rare exception represented in figures 10d, e, which models possibly the spherulite of plate IV, k, this one being simply twisted MBBA in glycerol and not a germ grown from its own isotropic phase. The only visible defects result from the coalescence of spherulites. The question of surface singularities can be considered from the existence of constraints on the angle α separating surface directors from the interface tangent plane. This problem was studied in a previous work [11].

If the angular conditions are not strict, and remain simply limited to the existence of an optimal angle, there is no surface discontinuities. If these angular conditions are strict, discontinuities exist in the form of either a closed line or of two singular points or both. The condition for having a surface line of discontinuity is the existence of a limiting angle α_L such as $0 < \alpha_L < \alpha < \pi/2$. Thus, molecules cannot be parallel to the interface except along the line of discontinuity. The condition for having surface singular points is the existence of an angle α_p such as $0 < \alpha < \alpha_p < \pi/2$. The simultaneous presence of points and lines corresponds to the existence of two limiting angles α_L and α_p such as $0 < \alpha_L < \alpha < \alpha_p < \pi/2$ [11].

It appears therefore that the only eventual singularities lie at the interface; this corresponds probably to the lowest energy configuration as suggested by Stein *et al.* [30] who compared structures and defects in ^{3}He-A and in cholesterics. When surface conditions are not strict in cholesteric droplets, and this can be the case, surface singularities are topologically avoidable. The presence of an optimal angle leads to a concentration along a line and around two narrow regions of the areas where molecules are either close to tangential or close to normal to the surface.

5.6 BULK DEFECTS. — The examination of biological analogues shows the absence of discontinuities in the bulk in general, but there are exceptions, the only one known being important. In Dinoflagellate chromosomes, one sees $\tau^{-\pi}$ disclinations and edge-dislocations, those showing either the configuration $\tau^{-\pi}\lambda^{+\pi}$ or $\lambda^{-\pi}\tau^{+\pi}$ [12]. However, these chromosomes are permanently condensed through the whole cell cycle and are not comparable to germs which grow without coalescence from the isotropic phase.

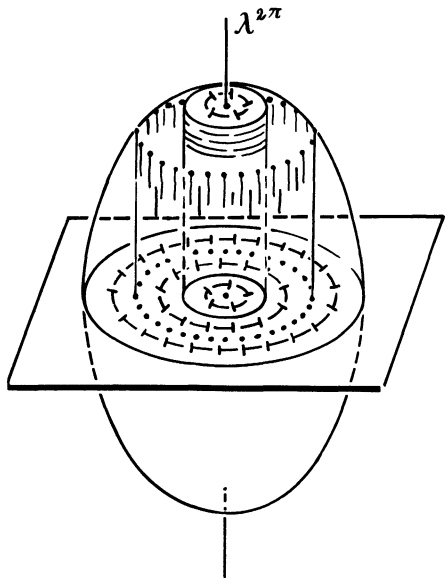

Fig. 21. — Cylindrical spherulite. Cholesteric layers are concentrically arranged around a $\lambda^{+2\pi}$ disclination. The cholesteric layers are cut normally by the equator plane and represented according to the nail convention.

It appears therefore that growth of cholesteric germs can work without defects affecting the continuity of the director distribution in the bulk and at the interface (when there are no strict angular conditions). This situation contrasts with that of true crystals whose growth depends on the presence of screw dislocations, which are found also in smectics and in columnar liquids. However, the formation of a disclination radius corresponds to the creation of a screw dislocation in the cholesteric layering. These screw dislocations are absent in germs showing a uniform orientation of layers.

6. Conclusions.

Cholesteric phases are thermodynamically nematic phases and, in these latter, screw dislocations cannot be defined. Cholesteric growth is similar to nematic growth from the isotropic phase and the absence of defects linked to the growth in cholesteric germs is therefore understood. However the cholesteric helicity leads to a discrete translation symmetry and, in the case of molecules lying mainly parallel to the interface, one gets a radial screw dislocation. Growth of germs with uniform distribution of cholesteric layers resembles rough growth in crystals, whereas growth of spherulites with concentric layers needs the presence of one screw dislocation at least and this recalls the facet growth of crystals facilitated by screw dislocations. There are no discontinuities of the molecular

orientation in the bulk, even if there is a radius of disclination, its core being a continuous structure. The only possible discontinuities in the bulk arise from germ coalescence. Interface angular conditions can lead, if very strict, to the presence of surface lines or/and points. This description of cholesteric spherulites could have a bearing in the study of defects of ^{3}He-A, because of the similarity of the order parameter.

Acknowledgments.

We would like to thank G. D. Mazur for discussions and advice on the manuscript.

References

[1] LEHMANN, O., *Flüssige Kristalle sowie Plastizität von Kristallen im allgemeinen Molekulare Umlagerungen und Aggregatzustandsänderungen* (Verlag von Wilhelm Engelman) 1904, 264 p.
[2] FRIEDEL, G., *Ann. Phys.* **18** (1922) 273.
[3] ROBINSON, C., *Trans. Faraday Soc.* **52** (1956) 571.
[4] ROBINSON, C., WARD, J. C., BEEVERS, R. B., *Diss. Faraday Soc.* **25** (1958) 29.
[5] KELLER, A., *J. Polym. Sci.* **39** (1959) 151.
[6] ROBINSON,C., *Molecular Crystals* **1** (1966) 467.
[7] ALBERTS, B., BRAY, D., LEWIS, J., RAFF, M., ROBERTS, K., WATSON, J. D., *Molecular Biology of the Cell,* (Garland Publishing, N. Y.) 1983, 1146 p.
[8] ROBINSON, C., *Tetrahedron.* **13** (1961) 219.
[9] RINAUDO, M., MILAS, M., *J. Polym. Sci.* **12** (1974) 2073.
[10] MARET, G., MILAS, M., RINAUDO, M., *Polymer. Bull.* **4** (1981) 291.
[11] BOULIGAND, Y., *J. Physique* **35** (1974) 215.
[12] LIVOLANT, F., *Europ. J. Cell. Biol.* **33** (1984) 300.
[13] BOULIGAND, Y., *C. R. Hebd. Séan. Acad. Sci.* **261** (1965) 3665, 4864.
[14] KLEMAN, M., FRIEDEL, J., *J. Physique Colloq.* **30** (1969) C4-43.
[15] BOULIGAND, Y., *J. Physique* **35** (1974) 959.
[16] BOULIGAND, Y., KLEMAN, M., *J. Physique* **31** (1970) 1041.
[17] SPENCER, M., FULLER, W., WILKINS, M. H. F., BROWN, G. L., *Nature* **194** (1962) 1014.
[18] SPENCER, M., POOLE, F., *J. Mol. Biol.* **11** (1965) 314.
[19] LAGERWALL, S. T., STEBLER, B., *Kosmos* (1979). *Svenska Fysikersamfundet* (1979) 115.
[20] FRIEDEL, G., GRANDJEAN, F., *Bull. Soc. Fr. Min.* **33** (1910) 192.
[21] GRANDJEAN, F., *Bull. Soc. Fr. Min.* **42** (1919) 42.
[22] OSEEN, C. W., *Trans. Faraday Soc.* **29** (1933) 883.
[23] FRANK, F. C., *Discuss. Far. Soc.* **25** (1958) 19.
[24] CLADIS, P. E., KLEMAN, M., *J. Physique* **33** (1972) 591 ; WILLIAMS, C. E., PIERANSKI, P. and CLADIS, P. E., *Phys. Rev. Lett.* **29** (1972) 90.
[25] MEYER, R. B., *Philos. Mag.* **23** 1973) 405.
[26] WILLIAMS, C., BOULIGAND, Y., *J. Physique* **35** (1974) 589.
[27] CLADIS, P. E., *Philos. Mag.* **29** (1974) 641.
[28] CLADIS, P. E., WHITE, A. E., BRINKMAN, W. F., *J. Physique* **40** (1979) 325.
[29] BOULIGAND, Y., *J. Physique* **34** (1973) 1011.
[30] STEIN, D. L., PISARSKI, R. D., ANDERSON, P. W., *Phys. Rev. Letters* **40** (1978) 1269.
[31] KELLER, A., *J. Polym. Sci.* **17** (1955) 291.
[32] KELLER, A., *J. Polym. Sci.* **17** (1955) 351.
[33] LOW, A., VESELY, D., ALLAN, P., BEVIS, M., *J. Materials Science* **13** (1978) 711.
[34] MICHEL-LEVY, MUNIER-CHALMAS, *Bull. Soc. Fr. Min.* **15** (1892) 159.
[35] WALLERANT, F., *Bull. Soc. Fr. Min.* **30** (1907) 43.
[36] GAUBERT, P., *Bull. Soc. Fr. Min.* **32** (1909) 421.
[37] BERNAUER, F., *Forschungen zur Kristallkunde* (Borntraeger, Berlin) **2** (1929).
[38] LISON, L., *Histochimie Animale. Méthodes et Problèmes* (Gauthier-Villars Paris) 1936, 320 p.
[39] STEWART, G. T., *Mol. Crystals* **1** (1966) 563.
[40] KENCHINGTON, W., FLOWER, N. E., *J. Microscopy* **89** (1969) 263.
[41] NEVILLE, A. C., LUKE, B. M., *J. Cell. Sci.* **8** (1971) 93.
[42] GUBB, D. C., Ph. D. Thesis, University of Bristol (1976).
[43] WHARTON, D. A., *Tissue and Cell.* **10** (1978) 647.
[44] PATTERSON, D. J., *Microbios.* **26** (1979) 165.
[45] DHAINAUT, A., PORCHET, M., *Biol. Cell.* **28** (1977) 241.
[46] AKAI, H., SATO, S., *Int. J. Insect. Morphol. Embryol.* **2** (1973) 207.
[47] BOULIGAND, Y., SOYER, M. O., PUISEUX-DAO, S., *Chromosoma* **24** (1968) 251.
[48] LIVOLANT, F., BOULIGAND, Y., *Chromosoma* **68** (1978) 21.
[49] GOURRET, J. P., *Biol. Cellulaire* **32** (1978) 299.
[50] COX, G., *Biol. Cell.* **31** (1978) 117.
[51] BRUGEROLLE, G., MIGNOT, J. P., *Biol. Cellulaire* **35** (1979) 111.
[52] ZUSMAN, D. R., CARBONELL, A., HAGA, J. Y., *J. Bacteriology* **115** (1973) 1167.
[53] DENEFLE, J. P., FAVARD, P., FAVARD, N., BOULIGAND, Y., LECHAIRE, J. P., *Biol. Cell.* **42** (1981) 21a.
[54] GOURRET, J. P., Thèse présentée à l'Université de Rennes le 4 nov. 1975.
[55] BOULIGAND, Y., in *Liquid crystalline order in polymers.* Editor A. Blumstein. (Academic Press Inc. New York, San Francisco. London.) 1978 Chap. VIII.
[56] LAPOINTE, J., MARVIN, D. A., *Molecular crystals and Liquid crystals* **19** (1973) 269.
[57] BOULIGAND, Y., *J. Physique Colloq.* **30** (1969) C4-90.